

**ULTRA-WIDE BAND BASED INDOOR POSITIONING SYSTEM USING
LATERATION METHODS**

**A THESIS SUBMITTED TO
THE GRADUATE SCHOOL OF NATURAL AND APPLIED SCIENCES OF
KARABUK UNIVERSITY**

BY

ANDAY DURU

**IN PARTIAL FULFILLMENT OF THE REQUIREMENTS FOR
THE DEGREE OF MASTER OF SCIENCE IN
DEPARTMENT OF
BIOMEDICAL ENGINEERING**

March 2018

I certify that in my opinion the thesis submitted by Anday DURU titled “ULTRA-WIDE BAND BASED INDOOR POSITIONING SYSTEM USING LATERATION METHODS” is fully adequate in scope and in quality as a thesis for the degree of Master of Science.

Prof. Dr. İdris KABALCI
Thesis Advisor, Department of Biomedical Engineering

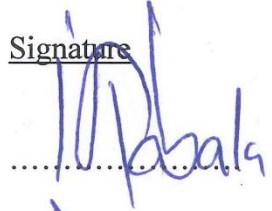


This thesis is accepted by the examining committee with a unanimous vote in the Department of Biomedical Engineering as a master thesis. Mar 16, 2018

Examining Committee Members (Institutions)

Signature

Chairman :Prof. Dr. İdris KABALCI (KBU)



Member :Assoc. Prof. Dr.Kemal POLAT (AIBU)



Member : Assist. Prof. Dr. Ahmet Reşit KAVSAOĞLU (KBU)



...../...../2018

The degree of Master of Science by the thesis submitted is approved by the Administrative Board of the Graduate School of Natural and Applied Sciences, Karabük University.

Prof. Dr. Filiz ERSÖZ
Head of Graduate School of Natural and Applied Sciences





“I declare that all the information within this thesis has been gathered and presented in accordance with academic regulations and ethical principles and I have according to the requirements of these regulations and principles cited all those which do not originate in this work as well.”

Anday DURU

ABSTRACT

M. Sc. Thesis

ULTRA-WIDE BAND BASED INDOOR POSITIONING SYSTEM USING LATERATION METHODS

Anday DURU

Karabük University

Graduate School of Natural and Applied Sciences

The Department of Biomedical Engineering

Thesis Advisor:

Prof. Dr. İdris KABALCI

March 2018, 52 pages

Global Positioning System is widely adopted technology and provides location data to the user all around the world. Most of the mobile and handheld devices have built-in GPS sensors. Although GPS are used in variety of tracking applications, their use is mainly based on outdoor environment and they can provide sufficient accuracy. Since GPS signals are disrupted and attenuated by materials between user and satellite, it is hard to locate user or asset in a building. In addition, there is no preferred technology like GPS to find position in indoor environment. At this point, there needs to be a different technology in indoor environment for both people and industry.

In this thesis, distance estimation methods, indoor positioning technologies and positioning algorithms are investigated with their advantages and limitations. After literature review, ultra-wideband technology has been chosen because of its very low

energy consumption, precision rate, robustness and low interference feature. The circuits have been designed and produced for creation of aimed network. Distance measurement tests have been conducted up to 20 m and the maximum mean absolute error has been found out as 3.67 cm. Three different positioning algorithms have been applied to the designed system and tests are carried out in 44 m² area. Maximum mean absolute error is measured as 59.93 cm among random position tests for Least Square Estimation positioning algorithm which brings the optimum results. The end product test results showed that the possibility of tracking in indoor environment with an error of under 60 cm depending on positioning algorithms. Results also state that ultra-wide band is an assuring technology for various indoor positioning applications.

Key Words : Wireless sensor network, UWB, Positioning system.

Science Code : 925.1.021

ÖZET

Yüksek Lisans Tezi

LATERASYON METOTLARINI KULLANARAK ULTRA-WIDE BAND TABANLI KAPALI ALAN KONUMLANDIRMA SİSTEMİ

Anday DURU

Karabük Üniversitesi

Fen Bilimleri Enstitüsü

Biyomedikal Mühendisliği Anabilim Dalı

Tez Danışmanı:

Prof. Dr. İdris KABALCI

Mart 2018, 52 sayfa

Global konumlandırma sistemleri geniş çapta kabul edilmiş bir teknolojidir ve bu sistem konum verisini kullanıcıya dünya çapında sağlayabilir. Hemen hemen bütün mobil ve elde tutulabilen cihazlar GPS sensörünü hazır olarak bulundurmaktadır. Global konumlama sistemi birçok takip uygulamalarında kullanılsa da daha çok açık alanlarda kullanımı yaygın olup, yeterli hassaslıkta ölçüm verirler. GPS sinyalleri kullanıcı ve uydu arasındaki malzemelerden kaynaklı olarak bozulduğu ve sönmüldüğü için yapı içerisinde bu sinyallerle konumlandırma işlemi zordur. Buna ek olarak, kapalı alanda konum bulmada GPS gibi kabul edilmiş bir teknoloji yoktur. Bu noktada endüstri ve insanlar için farklı bir kapalı alan konumlandırma teknolojisine ihtiyaç duyulmaktadır.

Bu tezde, mesafe tahmin metodları, kapalı alan konumlandırma teknolojileri ve konumlandırma algoritmaları avantajları ve kısıtlayıcı özellikleriyle araştırıldı.

Literatür taramasından sonra, ultra-wideband teknolojisi oldukça düşük enerji tüketimi, hassasiyet oranı, güçlü yapısı ve daha az etkileşme özelliklerinden dolayı seçildi. Devreler amaçlanan ağ örgüsünün oluşturulabilmesi için tasarlandı ve üretildi. 20 m'ye kadar mesafe testleri yapıldı ve en yüksek ortalama mutlak hata 3.67 cm olarak bulundu. Üç farklı konumlandırma algoritması tasarlanan sisteme uygulandı ve testler 44 m² alan içerisinde gerçekleştirildi. Rastgele konumlandırma testleri arasında optimum hata sonuçlarını veren en küçük kareler yöntemi ile yapılan konumlandırma testlerinin tamamında en yüksek 59.93 cm ortalama mutlak hata sonucu ölçüldü. Son ürün testleri algoritmalara bağlı olarak 60 cm'nin altında hata ile kapalı alanda konumlandırmanın mümkün olduğunu gösterdi. Sonuçlar gösteriyor ki ultra-wide band çeşitli kapalı alan konumlandırma sistemi uygulamaları için güvenilir bir teknolojidir.

Anahtar Kelimeler : Kablosuz sensör ağı, UWB, Konumlandırma sistemi.

Bilim Kodu : 925.1.021

ACKNOWLEDGMENT

The thesis and research was supported by Karabük University with KBÜBAP-17-YL-298 project number. Foremost, I would like to thank my advisor, Prof. Dr. İdris KABALCI for his interest and assistance in preparation of this thesis. Besides my advisor, I would also like to express my sincere gratitude to Eftâl ŞEHİRLİ and Kadir İLERİ for good discussions and help.

Completing my thesis developed my knowledge on applications on sensor based projects. Also, the researches and studies thought new technologies on indoor positioning and sensor networks.

This thesis would have never been possible without my family and parents.

CONTENTS

	<u>Page</u>
APPROVAL	ii
ABSTRACT.....	iv
ÖZET	vi
ACKNOWLEDGMENT	viii
CONTENTS.....	ix
LIST OF FIGURES	xi
LIST OF TABLES	xiii
ABBREVIATIONS INDEX.....	xiv
CHAPTER 1	1
INTRODUCTION	1
1.1. BACKGROUND	1
1.2. AIM.....	1
1.3. THESIS OUTLINE.....	2
CHAPTER 2	3
LITERATURE REVIEW	3
2.1. DISTANCE ESTIMATION METHODS	3
2.1.1. Angle of Arrival	3
2.1.2. Time of Arrival.....	4
2.1.3. Time Difference of Arrival.....	4
2.1.4. Received Signal Strength Indicator	5
2.2. POSITIONING TECHNOLOGIES	6
2.2.1 RF Based Positioning	6
2.2.2. Other Positioning Technologies	9
2.3. POSITIONING ALGORITHMS	10
2.3.1. Trilateration Algorithm	11
2.3.2. Least Square Estimation Algorithm	15
2.3.3. Centroid Positioning Algorithm	16

	<u>Page</u>
CHAPTER 3	17
THEORETICAL BACKGROUND.....	17
3.1. THE SYSTEM MODEL	18
3.1.1 Ultra-Wide Band Transceiver.....	18
3.1.2 Atmel Microcontroller.....	22
 CHAPTER 4	 27
THE SYSTEM DESIGN	27
4.1. CIRCUIT DESIGN	27
4.2. PRINTED CIRCUIT BOARD	28
4.2.1. UV Light Box	30
4.3. SOFTWARE DESIGN.....	35
4.3.1. Anchors and Tag.....	35
4.3.2. UV Light Box	36
4.3.3. Data Acquisition and Calculation.....	37
 CHAPTER 5	 38
RESULTS AND DISCUSSION	38
5.1. DISTANCE MEASUREMENT TESTS	38
5.1.1. Measurements up to 5-meter	39
5.1.2. 4-meter measurement	40
5.1.3. 6-meter measurement	42
5.1.4. 10-meter measurement	43
5.1.5. 15-meter measurement	44
5.1.6. 20-meter measurement	46
5.2. POSITION ESTIMATION	48
5.3. CONCLUSION	48
 REFERENCES	 50
RESUME	52

LIST OF FIGURES

	<u>Page</u>
Figure 2.1. Basic distance estimation scheme with AOA.....	4
Figure 2.2. Trilateration with three reference points	12
Figure 2.3. Concept of the centroid based IPS.....	16
Figure 3.1. Two way ranging concept	20
Figure 3.2. Discovery and Ranging phase	21
Figure 3.3. Message encodings on UWB ICs	21
Figure 3.4. Block diagram of the ATmega328p.....	22
Figure 3.5. SPI bus topologies a) Point to point topology b) Master connection to multiple slaves.	23
Figure 3.6. SPI transfer modes.....	24
Figure 3.7. I ² C connection to multiple slaves	25
Figure 3.8. Data transaction cycle in I ² C.	25
Figure 3.9. Data transmission frame	26
Figure 4.1. Connection schematic with microcontroller	28
Figure 4.2. a) Anchor and Tag circuit design, b) DWM1000 module extension..... board.	28
Figure 4.3. Relationship between cross section area and maximum current carrying capacity and temperature rise stated by IPC.	29
Figure 4.4. LED connection schematic.....	31
Figure 4.5. UV Box control unit design.....	31
Figure 4.6. Designed LED driver circuit.	32
Figure 4.7. Typical transfer characteristics of IRL540N	33
Figure 4.8. a) Clean copper plates b) Copper plate with dry photosensitive layer. .	34
Figure 4.9. a) UV LED control unit b) Circuit drawing on transparent paper.....	34
Figure 4.10. a) Circuit drawing exposure to the copper plate, b) After NaOH..... application to the copper plate.....	34
Figure 4.11. The PCBs after etching and drilling processes.....	34
Figure 4.12. Flow chart of the algorithm.	35

	<u>Page</u>
Figure 5.1. UWB based two-way communication system.....	38
Figure 5.2. Standard deviation with respect to real distance.	39
Figure 5.3. MAE with respect to real distance.....	40
Figure 5.4. Distance measurements between chips and ground with laser meter....	40
Figure 5.5. Results from 4-meter distance estimation test over time.....	41
Figure 5.6. Elapsed time histogram for 4-meter distance estimation test.....	41
Figure 5.7. Results from 6-meter distance estimation test over time.....	42
Figure 5.8. Elapsed time histogram for 6-meter distance estimation test.....	42
Figure 5.9. Results from 10-meter distance estimation test over time.....	43
Figure 5.10. Elapsed time histogram for 10-meter distance estimation test.....	43
Figure 5.11. Results from 15-meter distance estimation test over time.....	44
Figure 5.12. Elapsed time histogram for 15-meter distance estimation test.....	45
Figure 5.13. Results from 20-meter distance estimation test over time.....	46
Figure 5.14. Elapsed time histogram for 20-meter distance estimation test.....	46
Figure 5.15. Positioning error with respect to random positions.....	47

LIST OF TABLES

	<u>Page</u>
Table 2.1. Comparison of active RSSI based technologies.	8
Table 3.1. Comparison of wireless technologies for positioning.....	18
Table 5.1. Distance measurement results.....	47



ABBREVIATIONS INDEX

ABBREVIATIONS

GPS	: Global Positioning System
RSSI	: Received Signal Strength Indicator
RFID	: Radio Frequency Identification
RF	: Radio Frequency
TOF	: Time of Flight
UWB	: Ultra-Wide Band
TOA	: Time of Arrival
AOA	: Angle of Arrival
TDOA	: Time Difference of Arrival
SPI	: Serial Peripheral Interface
I ² C	: Inter-Integrated Circuit
SS	: Slave Select
SCLK	: Clock Signal
MISO	: Master In Slave Out
MOSI	: Master Out Slave In
CPOL	: Clock Polarity
CPHA	: Clock Phase
SDA	: Serial Data
SCL	: Serial Clock
MSB	: Most Significant Byte
LSB	: Least Significant Byte
WSN	: Wireless Sensor Network
IC	: Integrated Circuit
PCB	: Printed Circuit Board
UV	: Ultra Violet
LED	: Light Emitting Diode

LCD : Liquid Crystal Display
IDE : Integrated Development Environment
LSE : Least Square Estimation
MAE : Mean Absolute Error



CHAPTER 1

INTRODUCTION

1.1. BACKGROUND

Technological advances established many applications to ease both daily life and industry. Improvements in accurate localization systems enable to access navigation information around the world. GPS is commonly used method under outdoor environment. In this system, satellites transmit orbital parameters to GPS receivers on earth and these incoming signals are used by receivers to calculate location information of the device. Most of the mobile and handheld devices have built-in GPS sensors and they provide desired location data to users. Although GPS helps users to find location of intended places in outdoor environment, it has limitations in indoors. The main reason for the limitation is that GPS requires Line-of-Sight (LOS) signal propagation. Thus, indoor positioning systems (IPS) have been gained attention from researchers to cover LOS requirement and provide solutions. Although, there is no widely adopted IPS yet, many available technologies enable various solutions. Each one has its own advantages and limitations for monitoring applications.

1.2. AIM

IPS allows location based applications to work properly inside buildings. Since GPS technology could not supply desired precision in indoor environment, there has been many positioning systems developed based on different technologies to solve localization problem. The aim of the thesis is to create low-power, low-cost, easy to deploy and precise system for indoor use. Implementation possibilities include locating medical equipment, tracking stocks in a warehouse, guiding passengers for transport points in an airport, assisting to the needed store in a shopping mall etc. [1].

Further measurements with different distances are going to be held after the system is designed. Trilateration, Least Square Estimation and Centroid positioning algorithms are going to be applied to provide realistic information. Results are also going to be analyzed to discuss and compare the accuracy between different algorithms.

1.3. THESIS OUTLINE

First chapter of the thesis focuses on the problem that GPS does not give precise measurements and there needs to be another solution for positioning inside buildings. Second chapter of the thesis reviews literature to choose and design reliable system. Then, background of the designed system is explained in the third chapter of the thesis. Fourth chapter of the thesis informs about the evaluation of the system design. Ranging model of the tracking system is established and Trilateration, Least Square Estimation and Centroid Method positioning algorithms are applied in this chapter. The fifth chapter provides results of both distance measurements and position estimations with error calculations. Moreover, the ideas are shared to improve the current study.

CHAPTER 2

LITERATURE REVIEW

In this chapter, position estimation progress is explained by reviewing three stages. In the first stage, distance estimation methods are investigated. The second stage provides information about indoor positioning technologies. The final stage is the positioning algorithms to estimate position for intended area. All the stages must be considered to design a system with good accuracy.

2.1. DISTANCE ESTIMATION METHODS

This section provides information about distance estimation methods. If distance can be estimated by tag itself, then it is called self-positioning. On the other hand, if distance is estimated by a central unit, then it is called remote positioning. Estimation methods can be classified in 4 categories: Angle of Arrival (AOA), Time of Arrival (TOA), Time Difference of Arrival (TDOA) and Received Signal Strength Indicator (RSSI).

2.1.1. Angle of Arrival

The angle value from different nodes are used for determination of the seeking point, tag. Two reference points can supply necessary geometric intersection point of tag position. Reducing the reference points decrease the cost of application, but it is also going to decrease accuracy. In this method, there is no need for time synchronization between measuring units. However, calculation of the angle of an incoming signal is more complex than time stamping method [2]. Figure 2.1 demonstrates the basic working mechanism with AOA method. Received signal strength ratio between two directional antennas or multiple antenna array may be used for AOA determination. Accurate angle estimation is complex and challenging for this estimation type.

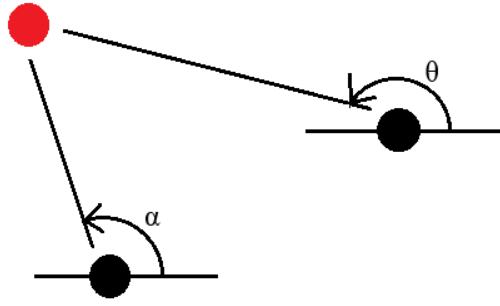


Figure 2.1. Basic distance estimation scheme with AOA.

2.1.2. Time of Arrival

Another position estimation method uses arrival time of the signal which is sent from reference point. In this form, transmitter sends a timestamp of the current time to the receiver and then receiver calculates the time difference. The time difference of signal sending and receiving is also called as Time of Flight (TOF). Ranging operation consist of only one transmission. Since the travel time of the RF signal and speed of light is known, the distance between transmitter and receiver can be calculated. TOA measurement highly depends on the clock accuracy in the receiver and transmitter chips. Clock drift of 1 ns results around 30 centimeters error in the application [2].

2.1.3. Time Difference of Arrival

In TDOA method, tag location is at intersections of hyperboloid or a hyperbola that are generated with the two sensors as foci. The location is calculated by the differences of arrival times measured on transmission paths. In TOA, location estimations are determined by the points of intersection of circles whose centers are located at the fixed points and the radius are estimated distances to the target. In this method, unknown tag position given in Eq. 2.1 and anchor positions, which are reference points, are given in Eq. 2.2 where M is the number of anchors.

$$E = [x^0, y^0]^T \quad (2.1)$$

$$s_i^0 = [x_i^0, y_i^0]^T \quad i = 1, 2, \dots, M \quad (2.2)$$

The tag location can be determined by the time differences between tag and reference points. TDOA is expressed in Eq. 2.3 where t_i represents the signal arrival time to the i^{th} sensor and t_1 is the time of arrival to the assumed “Anchor 1” point.

$$\Delta t_{i1} = t_i - t_1 \quad (2.3)$$

Then, it is possible to get Euclidean range distances by utilizing speed of light c , and time difference data (Eq. 2.4).

$$r_{i1}^0 = c\Delta t_{i1} \quad (2.4)$$

Distance difference equation with known anchor locations “ i ” and “ 1 ” can be written as Eq. 2.5 to determine tag’s location,

$$d_{i1} = \sqrt{(x_i^0 - x^0)^2 + (y_i^0 - y^0)^2} - \sqrt{(x_1^0 - x^0)^2 + (y_1^0 - y^0)^2} \quad (2.5)$$

Tag location can be computed by TDOA method [3]. However, positioning error may arise because of the coverage area and error in clock which is used to represent TOA at each anchor.

2.1.4. Received Signal Strength Indicator

Signal strength between transmitter and receiver indicated by the power value. Power of the signal decreases with greater distance, so RSS value can be classified as positioning parameter. This approach uses at least three nodes for determining position by trilateration method. However, RSSI value fluctuates because of the propagation mechanism such as reflection, scattering and diffraction [4]. Therefore, the received power estimation is generally modelled with algorithms to create more reliable results. Although RSSI is already adapted in most of the wireless protocols, this type of application is generally used when the accuracy is not demanded too much.

2.2. POSITIONING TECHNOLOGIES

There are numerous indoor positioning solutions based on different technologies. This section provides information about main indoor positioning systems with their downsides and advantages. Radio Frequency Identification Based (RFID), Wi-Fi, Bluetooth, ZigBee, Ultrasonic, Ultra-Wideband based Radio Frequency (RF) solutions are investigated in the first part. The second part includes various positioning technologies. Camera, visible light, dead reckoning based indoor positioning technologies are introduced in the second part.

2.2.1 RF Based Positioning

Among RF based indoor positioning solutions, distance can be estimated by Received Signal Strength Indicator (RSSI) and/or time-based indicators. RSSI is a measurement that indicates the power level of received signal. The positioning algorithm uses the signal strength to measure distance between two transceivers. Although RSSI value is easy to use for positioning algorithms, the RSSI data could be uncertain and may fluctuate over time because of variety of reasons which are explained in the next chapters [13]. On the other hand, time based indicators use signal propagation time. Precise clocks are significant to provide accurate distance estimations.

RFID Based Positioning

RFID tags can be classified by the method of powering them. Active tags include battery and have the capability of powering the circuit. By this way, it is possible to send high level signals as a response of low level reader signals. RSSI is the measure of distance in this technology. There are various problems about radio wave propagation in indoor environments. For example, absorption, diffraction, rare LOS path and reflection [5]. Therefore, environmental factors such as people, objects, walls affect RSSI value. On the other hand, a passive tag does not have internal battery. Predefined points are used to track location for seeking point. Although they are cheap in price, their use can be advantageous in some cases. Semi-passive tags

are similar to passive tag, but the main difference is that battery is not used for generating a response message. Powering the internal circuitry which is not related to tag is the reason to have an internal battery. Specific item or equipment tracking with given parameters is easier to apply for this technology.

Wi-Fi Based Positioning

Wi-Fi is a radio-frequency based positioning system and system measures RSSI to measure distance value. Although it has diverging advantages such as high bandwidth, different frequency bands (2.4, 3.6, 5 GHz) and adoption, there are also disadvantages as the same with RSSI based positioning systems. Since most of the mobile devices already has built-in Wi-Fi sensors, extra hardware cost will be minimum. However, accuracy is very limited with this positioning technology. Therefore, the system needs extra algorithms or hardware to make it good enough to use [6]. A hybrid system can be considered Wi-Fi with GPS and it can be used to get indoor and outdoor location data.

Bluetooth Based Positioning

Bluetooth also estimates the position of tag in similar ways with Wi-Fi, but it uses different frequency band (2.4Ghz). RSSI value is the estimation method and mentioned disadvantages also apply for Bluetooth based positioning systems. Since most of the cell phones has Bluetooth sensors inside, reference points need to be installed for better accuracy. Bluetooth technology has better resolution than Wi-Fi [7]. Thus, Bluetooth reference points is a must and multiples of them should be placed when the area increases.

ZigBee Based Positioning

Positioning system with ZigBee technology also stands on RSSI measurements. The issue for Radio Frequency (RF) signal behavior applies for this technology. It operates in 2.4GHz frequency band. One of the papers proposed that average absolute error can be under 3m with dynamic calibration [8]. Since RSSI value can

vary considerably with environmental factors, it is better to use for home automation, industrial automation, smart monitoring applications because of the power consumption rate, network size and network architecture. Table 2.1 compares available active RSSI based technologies.

Table 2.1. Comparison of active RSSI based technologies [9].

	Wi-Fi	Bluetooth	ZigBee
<i>Protocol</i>	802.11	802.15.1	802.15.4
<i>Power Consumption</i>	High	Low	Very Low
<i>Range</i>	100 m	10 m	10 – 100 m
<i>Bandwidth</i>	22 MHz	1 MHz	0.3/0.6 MHz – 2 MHz
<i>Network Size</i>	2007	8	> 65000
<i>Application Focus</i>	Speed	Cable Replacement	Automation

Ultrasound Based Positioning

In this method, ultrasonic sound waves are sent by a transmitter and then the signals are picked up by a receiver node. TOF data is used for distance estimation. Measurement with ultrasonic waves can achieve millimeter accuracy with a range of 6m. Unfortunately, undesirable phenomena can affect ultrasonic waves such as crosstalk, echo and jamming [10, 11].

Ultra-Wide Band Based Positioning

Large bandwidth signals allow transmission of short duration high energy pulses. Since it is possible to sense pulses as high as 20 times in a second, TOF and TOA positioning techniques can be applied. Therefore, high time resolution improves the accuracy of indoor positioning systems. Thus, it is possible to reach very good accuracy under 20cm [12]. As a result of large spectrum, Ultra-Wide Band (UWB) signals can penetrate through objects such as walls, doors etc. Since the energy of signal is dispersed over a broad frequency range, time frame can be kept compact without exceeding the energy density limits which in turn compresses the edge used for determining the receive time, allowing for very accurate time-stamping of incoming messages. High energy signals provide excellent scalability, and the

technology offers reduced complex processing of the obtained results [2]. The range and offered accuracy gives very promising results for indoor positioning algorithms. On the other hand, the UWB chips are not implemented on mobile devices and they are relatively expensive products. As the chips are produced in large scales, they will possibly supply the indoor positioning needs for various industries.

2.2.2. Other Positioning Technologies

This section provides information about positioning technologies that does not fit in one category. These methods have different mechanisms to locate moving objects. They each have its own advantages and disadvantages.

Camera Based Positioning

In this technique, camera is used to capture images and most of the cameras are useful for mapping. Since existing cameras can acquire images, data on those images are useful to differentiate objects or person. Also, tag does not have to carry any circuit for tracking. Image processing is required to measure distance and complex environments requires complex algorithms to detect target. Larger field of view and greater pixel density gives better data for processing. However, there are some issues about the camera based positioning systems. Tracked person should be in line of sight for processing, otherwise, the image is useless. Therefore, multiple cameras should be installed for increasing accuracy and line of sight. The deployment price gets higher as the number of cameras increases. Another problem is privacy concern. Tracking and recording image has a potential of unethical behavior, so it is undesirable for public applications.

Visible Light Communication

Visible light can be used for data transaction, so there are variety of application areas such as security, body area networks and indoor navigation applications. This technology uses visible light between 375 – 780 nm for data transaction. The system works by detecting coded emitted light. The stationary emitters send a message

including position data by blinking and target can see location of himself. However, line of sight is needed for this application and extra hardware should be deployed.

Dead Reckoning

This technique uses Inertial Measurement Unit (IMU) which includes accelerometer, gyroscope and magnetometer for positioning. The last known position is combined with accelerometer and angular velocity data and the new position is estimated. Since every position change depends on the previous data, the error increases with movement. Thus, frequent calibration is needed for this application. IMU data is better to use in hybrid systems for increasing the accuracy of positioning technologies.

2.3. POSITIONING ALGORITHMS

There are various algorithms to calculate position some of which are proximity algorithm, triangulation algorithm and fingerprinting algorithm. Proximity algorithm basically uses the connectivity principle. After relative position is determined by the power of RSSI, number of anchors is the main factor that affects the accuracy. Triangulation algorithm uses geometry to calculate the position of tag. It has two division as lateration and angulation. Lateration algorithm receives range data by the propagation of time and it needs at least three anchors to locate tag. Also, there needs to be $N+1$ sensors for N dimensional places. Angulation algorithm uses the same principle with AOA. Fingerprinting is a popular algorithm which collects signal data and creates a database. This database comprises training phases by matching real coordinates and signal characteristics. The second phase locates by measuring signal values and searches database for nearest points. On the other hand, it has training problems due to unstable signals [13]. Three different lateration algorithms are investigated with their mathematical background.

2.3.1. Trilateration Algorithm

Spatial coordinate calculation of an unknown point regarding distance measurements of three reference points is known as trilateration. The system uses trilateration to calculate position of tag. Once the distance measurements are received, the location is calculated. If the unknown point is (x, y) , known points are (x_i, y_i) and r_i represents the radius of the circle. Therefore, we have three sets of circle equations with known radius parameter and anchor locations (Eq. 2.6).

$$\begin{aligned}(x - x_1)^2 + (y - y_1)^2 &= r_1^2 \\(x - x_2)^2 + (y - y_2)^2 &= r_2^2 \\(x - x_3)^2 + (y - y_3)^2 &= r_3^2\end{aligned}\tag{2.6}$$

Expanding out the squared parameters gives Eq. 2.7,

$$\begin{aligned}x^2 - 2x_1x + x_1^2 + y^2 - 2y_1y + y_1^2 &= r_1^2 \\x^2 - 2x_2x + x_2^2 + y^2 - 2y_2y + y_2^2 &= r_2^2 \\x^2 - 2x_3x + x_3^2 + y^2 - 2y_3y + y_3^2 &= r_3^2\end{aligned}\tag{2.7}$$

Subtracting second equation from the first one gives Eq. 2.8,

$$(-2x_1 + 2x_2)x + (-2y_1 + 2y_2)y = r_1^2 - r_2^2 - x_1^2 + x_2^2 - y_1^2 + y_2^2\tag{2.8}$$

Likewise, subtracting the third equation from the second one gives Eq.2.9,

$$(-2x_2 + 2x_3)x + (-2y_2 + 2y_3)y = r_2^2 - r_3^2 - x_2^2 + x_3^2 - y_2^2 + y_3^2\tag{2.9}$$

The system has been re-created with two unknowns, and the solution is Eq. 2.10,

$$\begin{aligned}Ax + By &= C \\Dx + Ey &= F\end{aligned}\quad \begin{aligned}x &= \frac{CE - FB}{EA - BD} \\y &= \frac{CD - AF}{BD - AE}\end{aligned}\tag{2.10}$$

Through solving the equation, position of tag is calculated. Figure 2.2 shows an example of anchors with distances to the tag.

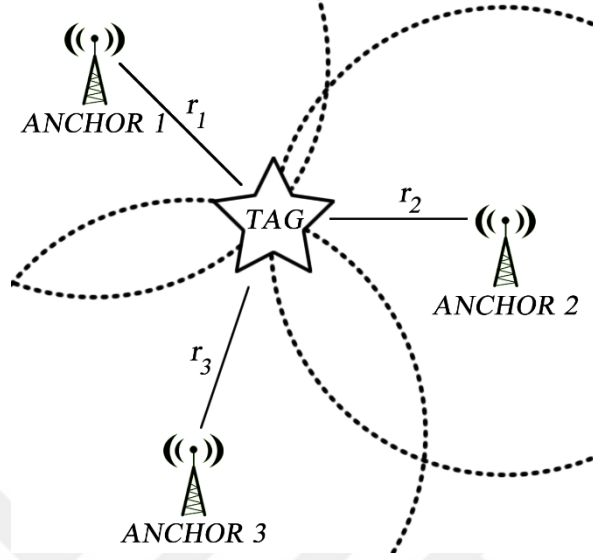


Figure 2.2. Trilateration with three reference points.

A. Norrdine proposed trilateration algorithm for UWB indoor positioning system with low computational complexity. The method uses nonlinear elements of the equation as additional unknowns. Since the calculation are going to be implemented on the system, low computational complexity is necessary for fast and accurate data acquisition. The paper describes the calculation with three given reference points which are $P_1(x_1, y_1, z_1)$, $P_2(x_2, y_2, z_2)$, $P_3(x_3, y_3, z_3)$ with the range data s_1, s_2, s_3 to the point N.

Coordinates of N is equal to the solution of following quadratic Eq. 2.11,

$$\begin{aligned} (x - x_1)^2 + (y - y_1)^2 + (z - z_1)^2 &= s_1^2 \\ (x - x_2)^2 + (y - y_2)^2 + (z - z_2)^2 &= s_2^2 \\ (x - x_3)^2 + (y - y_3)^2 + (z - z_3)^2 &= s_3^2 \end{aligned} \quad (2.11)$$

Re-arranging the equation gives Eq. 2.12,

$$\begin{aligned} (x^2 + y^2 + z^2) - 2x_1x - 2y_1y - 2z_1z &= s_1^2 - x_1^2 - y_1^2 - z_1^2 \\ (x^2 + y^2 + z^2) - 2x_2x - 2y_2y - 2z_2z &= s_2^2 - x_2^2 - y_2^2 - z_2^2 \\ (x^2 + y^2 + z^2) - 2x_3x - 2y_3y - 2z_3z &= s_3^2 - x_3^2 - y_3^2 - z_3^2 \end{aligned} \quad (2.12)$$

Putting the equations in matrix form represents Eq. 2.13,

$$\begin{bmatrix} 1 & -2x_1 & -2y_1 & -2z_1 \\ 1 & -2x_2 & -2y_2 & -2z_2 \\ 1 & -2x_3 & -2y_3 & -2z_3 \end{bmatrix} \begin{bmatrix} x^2 + y^2 + z^2 \\ x \\ y \\ z \end{bmatrix} = \begin{bmatrix} s_1^2 - x_1^2 - y_1^2 - z_1^2 \\ s_2^2 - x_2^2 - y_2^2 - z_2^2 \\ s_3^2 - x_3^2 - y_3^2 - z_3^2 \end{bmatrix} \quad (2.13)$$

The equation is set in the form of Eq. 2.14,

$$A_0 \cdot \mathbf{x} = \mathbf{b}_0 \quad (2.14)$$

Since the constraint, $\mathbf{x} \in E$, the equation is set in the form of Eq. 2.15,

$$E = \{(x_0, x_1, x_2, x_3)^T \in \mathbf{R}^4 / x_0 = x_1^2 + x_2^2 + x_3^2\} \quad (2.15)$$

Assuming P_1, P_2, P_3 does not lie on a straight line, then constraints are given in Eq. 2.16,

$$\text{Range}(A_0) = 3 \text{ and } \dim(\text{Kern}(A_0)) = 1 \quad (2.16)$$

The general solution of the system is represented in Eq. 2.17, where x_p represents the particular solution, x_h is the solution of a homogenous system and the real parameter t . x_p and x_h can be calculated by Gaussian elimination method.

$$\mathbf{x} = \mathbf{x}_p + t \cdot \mathbf{x}_h \quad (2.17)$$

Calculating the real parameter t gives Eq. 2.18,

$$\begin{aligned} \mathbf{x}_p &= (x_{p0}, x_{p1}, x_{p2}, x_{p3})^T \\ \mathbf{x}_h &= (x_{h0}, x_{h1}, x_{h2}, x_{h3})^T \\ \mathbf{x} &= (x_0, x_1, x_2, x_3)^T \end{aligned} \quad (2.18)$$

Inserting into Eq. 2.17, the Eq. 2.19 is acquired,

$$\begin{aligned} x_0 &= x_{p0} + t \cdot x_{h0} \\ x_1 &= x_{p1} + t \cdot x_{h1} \end{aligned} \quad (2.19)$$

$$x_2 = x_{p2} + t \cdot x_{h2}$$

$$x_3 = x_{p3} + t \cdot x_{h3}$$

The constraint $x_0 = x_1^2 + x_2^2 + x_3^2$ gives the following Eq. 2.20,

$$x_{p0} + t \cdot x_{h0} = (x_{p1} + t \cdot x_{h1})^2 + (x_{p2} + t \cdot x_{h2})^2 + (x_{p3} + t \cdot x_{h3})^2 \quad (2.20)$$

Rearranging Eq. 2.20 gives Eq. 2.21,

$$t^2(x_{h1}^2 + x_{h2}^2 + x_{h3}^2) + t \cdot (2 \cdot x_{p1}x_{h1} + 2 \cdot x_{p2}x_{h2} + 2 \cdot x_{p3}x_{h3} - x_{h0}) + x_{p1}^2 + x_{p2}^2 + x_{p3}^2 - x_{p0} = 0 \quad (2.21)$$

The solutions of the quadratic Eq. 2.21 is calculated by Eq. 2.22,

$$t_{1/2} = \frac{-b \pm \sqrt{b^2 - 4ac}}{2a} \quad (2.22)$$

The solution of the system is written as Eq. 2.23,

$$x_1 = x_p + t_1 \cdot x_h \quad (2.23)$$

$$x_2 = x_p + t_2 \cdot x_h$$

The real part is going to be used when the multi-iteration problem cannot be solved. This approximation means that $x_{1/2} \in E$ is not met. The difference can be expressed as Eq. 2.24,

$$d = x_0 - (x_1^2 + x_2^2 + x_3^2) \quad (2.24)$$

Eq. 2.24 is the measure of solvability of the problem. x_0 , x_1 , x_2 and x_3 are the coordinates of x . Solution of the multilateration problem can be determined as Eq. 2.25,

$$N_1 = x_1 \cdot I \quad (2.25)$$

$$N_2 = x_2 \cdot I$$

I equal to Eq. 2.26,

$$I = \begin{bmatrix} 0 & 0 & 0 & 0 \\ 0 & 1 & 0 & 0 \\ 0 & 0 & 1 & 0 \\ 0 & 0 & 0 & 1 \end{bmatrix} \quad (2.26)$$

The method solves the problem without over determination [14]. Linear algebraic method decreases the computational complexity and makes it applicable for use in fast position calculations.

2.3.2. Least Square Estimation Algorithm

When more than three reference points are included in the algorithm, there needs to be an extensive solution. One of the widely used algorithm to solve over determined matrices is Least Square Estimation (LSE). Since the number of equations are greater than the unknown numbers, optimal position of tag can be calculated using LSE algorithm. Additional anchor points and its distances to tag are included in Eq. 2.27.

$$\begin{bmatrix} 1 & -2x_1 & -2y_1 & -2z_1 \\ 1 & -2x_2 & -2y_2 & -2z_2 \\ \vdots & \vdots & \vdots & \vdots \\ 1 & -2x_n & -2y_n & -2z_n \end{bmatrix} \begin{bmatrix} x^2 + y^2 + z^2 \\ x \\ y \\ z \end{bmatrix} = \begin{bmatrix} s_1^2 - x_1^2 - y_1^2 - z_1^2 \\ s_2^2 - x_2^2 - y_2^2 - z_2^2 \\ \vdots \\ s_n^2 - x_n^2 - y_n^2 - z_n^2 \end{bmatrix} \quad (2.27)$$

In this overdetermined estimation case, there is no solution. However, a meaningful approximate solution can be obtained by minimizing the following square error (Eq. 2.28).

$$\min \|Ax - \mathbf{b}\|^2 \quad (2.28)$$

Elements of A represents a matrix, and \mathbf{x} is a vector that needs to be solved to obtain position of tag. Distance equations between tag and anchors are included in vector \mathbf{b} . Sum of squares are written in Eq. 2.29 to determine least square estimator. Derivation of least square estimator gives Eq. 2.30.

$$\|Ax - \mathbf{b}\|^2 = (Ax - \mathbf{b})'(Ax - \mathbf{b}) = \mathbf{x}'A'A\mathbf{x} - 2\mathbf{x}'A'\mathbf{b} + \mathbf{b}'\mathbf{b} \quad (2.29)$$

$$2A'Ax - 2A'b = 0 \quad (2.30)$$

The derivatives are set to zero to minimize least square error. Therefore, the normal equation is obtained by solving Eq. 2.30 for x and Eq. 2.31 is obtained.

$$x = (A^T A)^{-1} A^T b \quad (2.31)$$

2.3.3. Centroid Positioning Algorithm

This method uses the center of a polygon to estimate position of tag. Range measurements determine radius of circles. Closest intersection points of circles define the corners of polygon. Thus, position of tag can be calculated by finding centroid of a polygon. Figure 2.3 shows the centroid positioning concept. The coordinates of tag location represented in Eq. 2.32 for a triangle. Then, the centroid of the triangle represents average coordinates of tag.

$$(x, y) = \left(\frac{x_1 + x_2 + x_3}{3}, \frac{y_1 + y_2 + y_3}{3} \right) \quad (2.32)$$

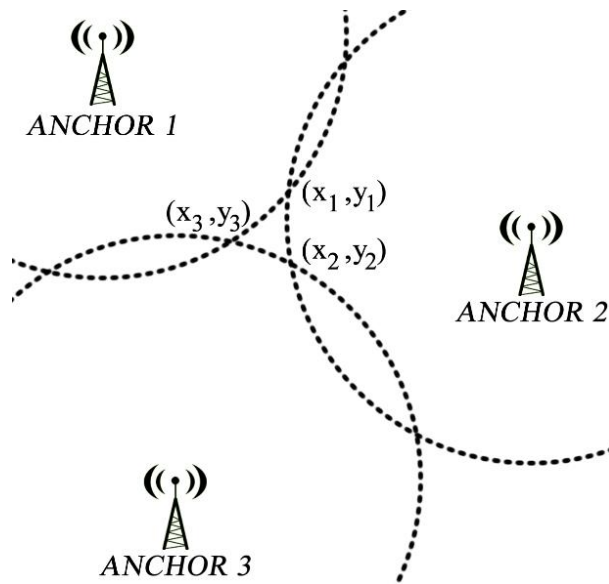


Figure 2.3. Concept of the centroid based IPS.

CHAPTER 3

THEORETICAL BACKGROUND

The recent studies, reviewed in the previous chapters, have provided very useful information about distance estimation methods, positioning technologies and positioning algorithms. Estimation methods are investigated for more accurate measurements. Moreover, comparisons between technologies assisted to choose and design better network for indoor positioning. In this part, the system background represented and explained step by step while creating aimed sensor network.

In information technology, a network is a series of nodes interconnected by communication paths for transmitting and receiving data. Networks can interconnect with other networks and contain sub-networks. Digital networks may consist of one or more routers that route data to correct user. Most sensor networks are heterogeneous meaning that there are nodes with different capabilities and requirements. In many cases, positioning of a sensor is another aspect apart from data acquisition. There are many technologies for indoor positioning as mentioned in Chapter 2.

It is possible to use different radio frequencies for indoor positioning such as Wi-Fi, ZigBee and UWB. However, ZigBee technology is useful for wireless control and monitoring solutions without extensive infrastructure wiring. Positioning with ZigBee technology is also possible when accuracy is not demanded too much. On the other hand, Wi-Fi technology provides longer communication distance than ZigBee and UWB technology. Complexity and energy consumption rates of Wi-Fi are much higher than that of ZigBee and UWB. However, both Wi-Fi and ZigBee technology have several meters accuracy when they applied for positioning. Compared to ZigBee and Wi-Fi technology, UWB offers significant advantages with respect to robustness, energy consumption and location accuracy [15].

The features of UWB states that it is a useful technology for indoor positioning. Table 3.1 compares features of wireless technologies for positioning. UWB has better location accuracy, low interference, low power consumption and medium data rate.

Table 3.1. Comparison of wireless technologies for positioning [15].

	Wi-Fi	ZigBee	UWB
<i>Data Rate</i>	High, 11 Mbps for 802.11b and 100+ Mbps for 802.11n	Low, 250 Kbps	Medium, 1 Mbps mandatory, up to 27 Mbps for 802.15.4a
<i>Transmission Distance</i>	Long, up to 100 meters	Short, several meters	Short, < 30 meters
<i>Location accuracy</i>	Low, several meters	Low, several meters	High, < 50 cm
<i>Power Consumption</i>	High, 500mW – 1W	Low, 20mW – 40mW	Low, 30mW
<i>Interference to other systems</i>	High	High	Low

3.1. THE SYSTEM MODEL

In the designed system, the features of UWB technology has been emerged among the other ones. Thus, UWB transceivers has been chosen to provide distance estimation data between sensors. The ranging model is explained in the subsection. Microcontroller must be included in the circuit design to initiate sensors, communicate and data collection. It is also possible to add different sensors and collect various data such as physiological, motion etc. Aimed system scenario measures distances and processes it to a central monitoring station and positioning algorithms are going to be applied.

3.1.1 Ultra-Wide Band Transceiver

UWB technology have gained widespread use in a variety of applications and getting more interest day by day because it has many advantages. Very precise location of tagged objects with low cost implementation is the most crucial one. Since UWB systems has noise like properties, it creates little interference to other systems. Thus, they are resistant to severe multipath and jamming, and have very good time-domain

resolution allowing for precise location and tracking. Various UWB wireless sensor network applications include locating and imaging of objects and environments, perimeter intrusion detection, video surveillance, in-vehicle sensing, outdoor sports monitoring, monitoring of highways, bridges, and other civil infrastructure, and so on [16]. Moreover, lots of applications exist in medicine which uses UWB to track and locate patients, personnel, assets etc. UWB technique achieves higher accuracy positioning than conventional wireless technologies (e.g. RFID, WLAN etc.) [17]. In this project, location aware Wireless Sensor Network (WSN) is created by a sensor which uses UWB technology. Mentioned sensor which is DW1000 designed as a transceiver for communication. Some of the key advantages of the UWB sensor are relatively low cost, low power, small form and robustness. Producing low cost sensor provides large number of nodes, so wide range area network can be created with relatively in an inexpensive way. Creating small device has the advantage of easy positioning and easy deployment procedure where the sensing actually takes place. Low power consumption property of the device operates device long times without any battery replacement. Robust sensor is required so that high quality of data communication can be guaranteed. However, the sensor has enough timing resolution capability because of the high frequency. Therefore, it can be used in two-way ranging systems or TDOA location systems for positioning. In addition, it has a precision rate of 10 cm and supports data rates of up to 6.8 Mbps. Two way ranging concept can be explained by the data acquisition of sensors. Determining TOF of signals between sensors gives information about distance between them. The distance formula between two objects can be expressed as,

$$\text{Distance} = \text{Speed of radio waves} \times \text{Time of Flight} \quad (3.1)$$

Timestamping with precise clock is also important factor to calculate precise TOF data. Timing while sending and receiving radio signals should also be progressed by the Integrated Circuit (IC). Two way ranging model applies for distance measurement between two UWB transceivers.

Two Way Ranging Concept: The anchor starts a transmission of a radio message1 to the tag and records its time of transmission (transmit timestamp) t1. Then, the tag

receives the message and transmits a response message (a radio message) back to the anchor after a delay t_{reply} . The anchor then receives this response and records a receive timestamp t_2 . This process is shown in the Figure 3.1.

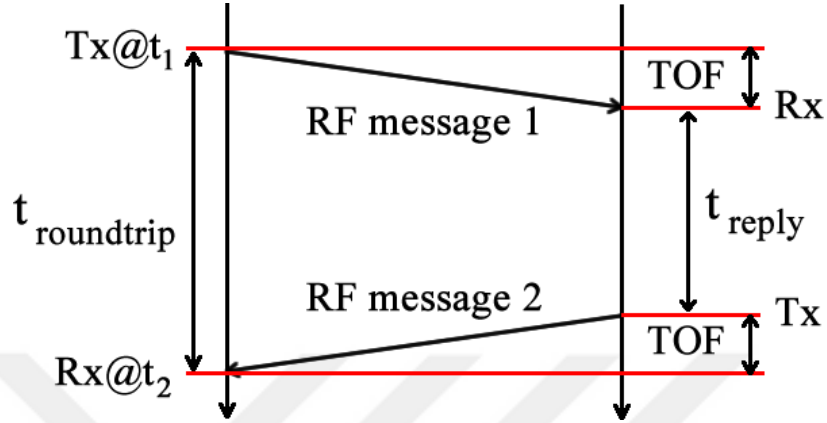


Figure 3.1. Two way ranging concept.

Now using the recorded timestamps t_1 and t_2 , the anchor can calculate the round-trip time $t_{roundtrip}$ and knowing the reply time in the tag, t_{reply} , the TOF can be determined by Eq. 3.2,

$$TOF = \frac{t_2 - t_1 - t_{reply}}{2} \quad (3.2)$$

If we assume the speed of radio waves through air is the same as the speed of light c , then the distance between the anchor and tag can be calculated by Eq. 3.3,

$$Distance = c \times \frac{t_2 - t_1 - t_{reply}}{2} \quad (3.3)$$

There are errors due to clock and frequency drift causing change in accuracy. However, error is going to be calculated after the overall system is designed.

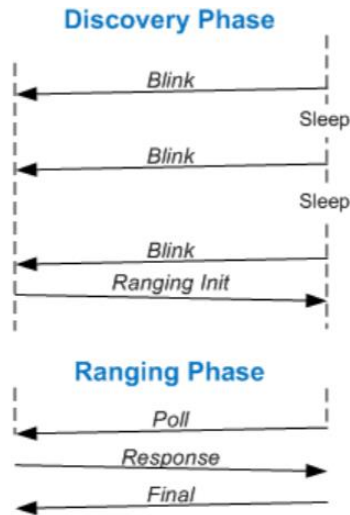


Figure 3.2. Discovery and Ranging phase [18].

The basic mechanism of messaging between transceivers in discovery and ranging phase is given in Figure 3.2. In the ranging application, Tag initiates the ranging by sending periodic blinks. The blink message includes the address of tag, then waits for a response from an anchor. Whenever anchor takes blink message, two way ranging communication starts by sending Ranging initialization message from anchor. This is the discovery phase of the modules and before the ranging phase starts. In the ranging phase, two-way ranging is executed by the tag sending Poll message, receiving the response message and then sending the Final message [35]. of Ranging message encodings are given in the Figure 3.3.

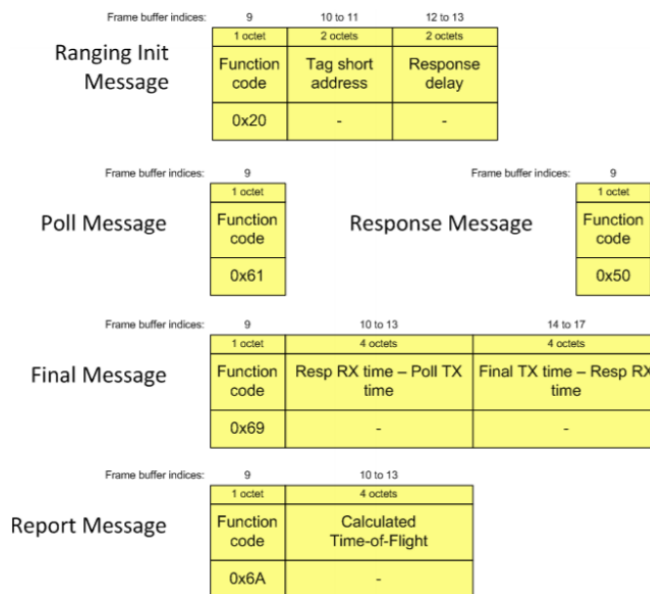


Figure 3.3. Message encodings on UWB ICs [35].

3.1.2 Atmel Microcontroller

Configuration and addressing of UWB modules must be programmed each time whenever the sensor needs to be in use. Also, sending and receiving data times should be acquired and calculated to find out distance. Therefore, microcontroller must be added in the system structure for communication between sensors and calculations. Since ATmega328p microcontroller is low-cost, low power and high-performance chip with sufficient pins for the project, it has been chosen for the application of system. This makes the project work even faster. Figure 3.4 shows the block diagram of the chip. The chip allows I²C and SPI communication at the same time and these two communication protocols are explained to understand data acquisition.

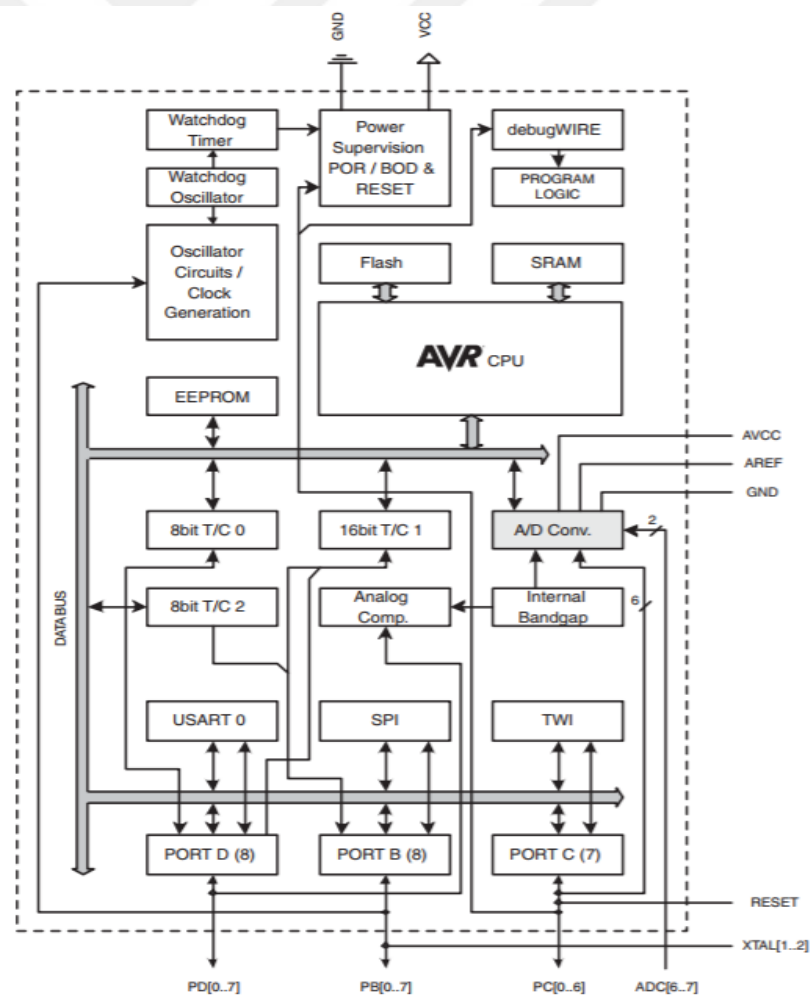


Figure 3.4. Block diagram of the ATmega328p [19].

Serial Peripheral Interface

SPI communication is quite straightforward protocol between two digital devices. It includes two data lines and two service lines.

- **SS** A Slave Select signal line allows or disallows slave to communicate with master.
- **SCLK** A clock signal is sent from the master to all slaves, so all the signals are synchronous to this signal.
- **MOSI** Master Out Slave In is the data transferring line from the master to slaves over this line.
- **MISO** Master In Slave Out is the data transferring line from slaves to master over this line.

In SPI, one central device initiates and controls all the communication. This means that it is a single-master communication protocol (Figure 3.5). If the master wants to send or request data from a slave, it selects a slave by pulling the corresponding SS line low. The second service line is clock signal, the frequency of the clock signal determines the data transfer speed. Therefore, synchronization of transfer speed between master and slave created. Operation modes and so number of connection may vary considering the type of sensor such as while communicating with read only or write only device.

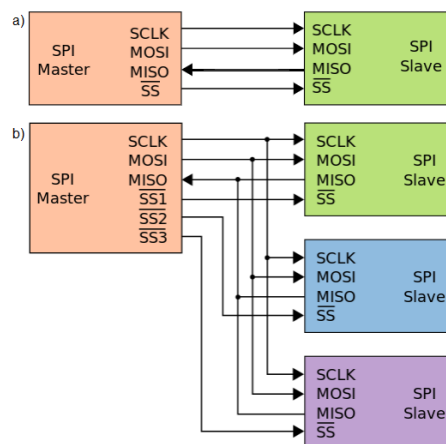


Figure 3.5. SPI bus topologies a) Point to point topology b) Master connection to multiple slaves.

Another important aspect is that transfer modes should be same between master and slave to make them speak same language. On the other hand, four transfer modes are available which defines clock format to be used. The format parameters are Clock Polarity (CPOL) and Clock Phase (CPHA). CPOL parameter inverts or non-inverts the clock polarity. CPHA parameter regulates the sampling phase. If CPHA is set to 0, then data is sampled on the first (leading) edge of the clock signal. In contrast, if CPHA is set to 1, the data will be sampled on the second (trailing) edge of the clock signal. As can be seen in Figure 3.6, data must be available before the clock signal rising or falling depending on the transfer mode.

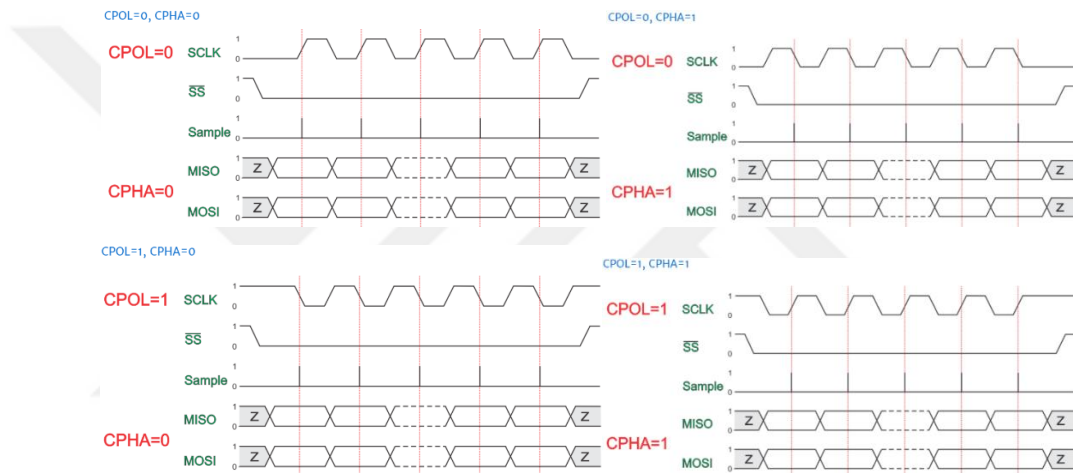


Figure 3.6. SPI transfer modes [20].

SPI protocol does not define any maximum data rate nor any particular addressing scheme. There is no acknowledgement mechanism for confirmation of data transfer.

Inter Integrated Circuit

I²C protocol requires two wires Serial Data (SDA) and Serial Clock (SCL) for connecting all the devices in the circuit (Figure 3.7). The data specification rates are between 100kb/s and 3.4Mb/s, respectively. In this protocol, any number of master can be connected to any number of slaves on these two signal lines and communicate with each other. Also, there is no need for SS line because of the communication technique. 7-bit unique slave address and start, direction of data, end, acknowledgement mechanism requires more bits to be transferred each time. These

active wires are bi-directional, so master and slave communicates on the same line. The data transfer starter is considered as master and all the other devices considered as slaves.

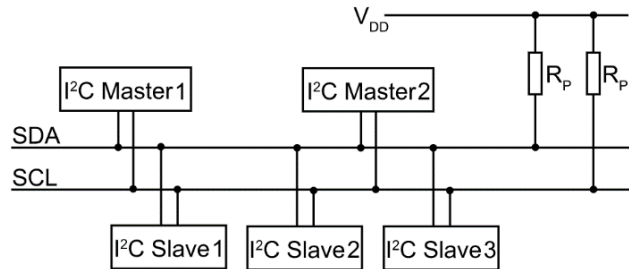


Figure 3.7. I²C connection to multiple slaves [21].

The devices on the line are connected to the bus via an open collector or open drain. This connection makes the device output either logic zero or nothing at all. If outputs of all devices are in high impedance state, two external pull-up resistors R_p holds the lines at high logic level (logic 1).

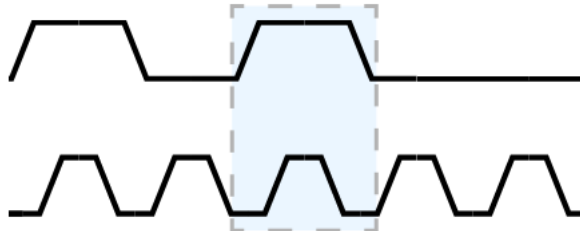


Figure 3.8. Data transaction cycle in I²C.

It is important to know that values on SDA line are changed when SCL line is low as the Figure 3.8 shows an example. When the SCL line is high, the receiver reads the data bit. At this point SDA line must be stable. Exception for this rule is the Start and Stop conditions. For a Start condition, The SDA line changes from one to zero leaving the SCL line high. After that, the master outputs zero on the SCL line to prepare the bus for the transmission. The first seven bits contain slave address will be sent after the start condition. The address is transmission is done sequentially, starting with Most Significant Byte (MSB) first with a Least Significant Byte (LSB) ending. Each slave must have a unique address to cancel conflicts. The transaction on

the Figure 3.9 has a slave address of 1010001 (0x51). The slaves without this address waits for a Stop condition. The eighth bit defines the direction of transmission (0=Write, 1=Read). The master can send first byte of the data after the acknowledgement. Then, the data acknowledged by slave. When the transmission session ends the master generates the stop condition and free the bus. Stop condition is created by the change of SDA from low to high while SCL line is high.

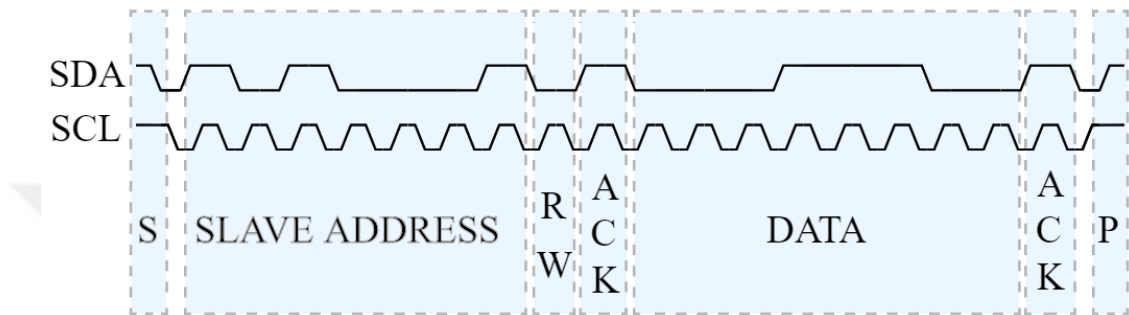


Figure 3.9. Data transmission frame [21].

CHAPTER 4

THE SYSTEM DESIGN

Indoor positioning has emerged in many applications for tracking people or stocks. For example, older people spend most of their time in indoor environment, some of them are living alone in their home. The report published by Australian Institute of Health and Welfare shows that most of the falls (>75%) occur within indoor environments. Therefore, it is essential to have powerful indoor-location-aware telehealth systems which are able to locate the positions of people indoor in the case of a medical emergency in order to summon immediate help [22]. The system design focuses on creating a robust indoor positioning system and testing different positioning algorithms. The advantages of UWB technology features directed to choose DWM1000 UWB transceivers. Performance, endurance, power consumption rate and peripheral features are directed to choose ATmega328p microcontroller for the communication between transceivers and microcontroller. Printed circuits are designed considering communication protocol, pin connections and size. UV light box was also designed and used to manage circuit drawings on copper plates. Software implementations are crucial steps for reliable distance calculations. Applied algorithms are going to provide realistic accuracy measure and inform about usefulness of the designed system. Circuit and software design and implementation processes are explained step by step to achieve and analyze the indoor positioning system.

4.1. CIRCUIT DESIGN

Anchors and tag must be designed considering pin connections of both microcontroller and DWM1000 which is UWB transceiver. Getting position data requires at least 3 reference points. Therefore, 4 reference points and 1 tag are produced for testing positioning algorithms. Anchors and tag have been connected to

microcontroller via SPI protocol. Connection scheme between microcontroller and UWB chip is shown in Figure 4.1.

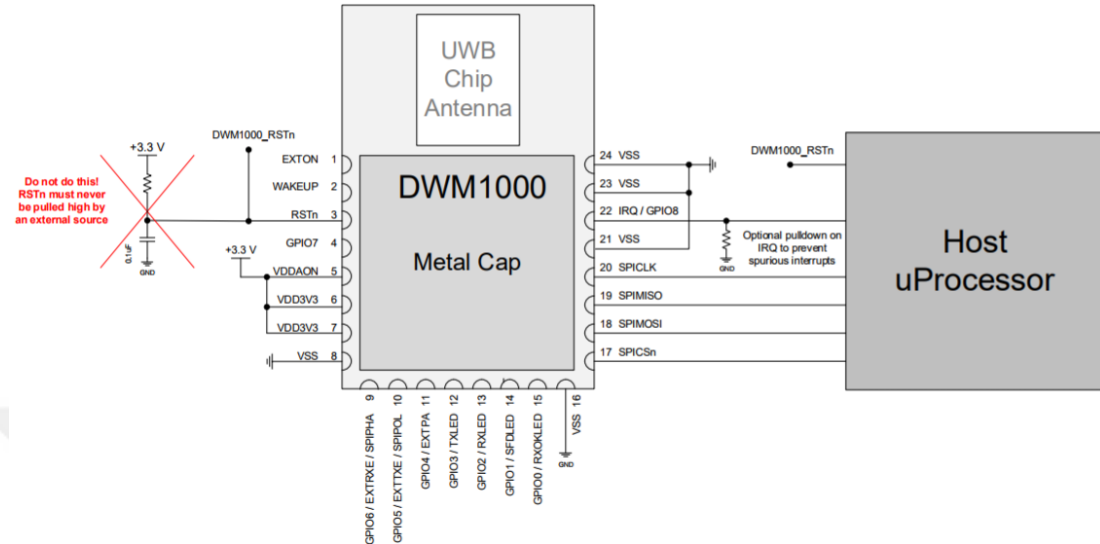


Figure 4.1. Connection schematic with microcontroller [23].

Printed Circuit Board (PCB) design has been created in Proteus software which is an electronic design automation program. The anchor and tag design is shown in Figure 4.2(a). Designed UWB module extension board for vertical position to the circuit can be seen in Figure 4.2(b).

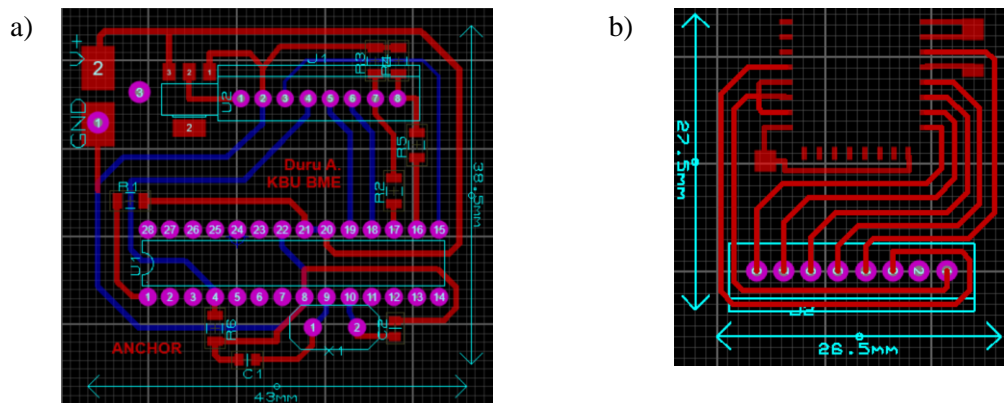


Figure 4.2. a) Anchor and Tag circuit design, b) DWM1000 module extension board.

4.2. PRINTED CIRCUIT BOARD

PCB is used to assemble electronic parts in a rigid manner. Circuitry should be designed in a computer aided design software and connections must be checked.

Also, size of materials which are going to be mounted on PCB must match with the design. Chip manufacturers provide datasheets for circuit designers. This sheet includes characteristics and physical size of the chip. Outside factors should also be known before selecting copper plate size. For example, battery connections or size of the case should be considered. Also, trace sizing is important factor because copper traces has resistance value in real world. While the current flows in copper, voltage drops and power dissipation may occur. Determining current carrying capacity and sizes of etched copper conductors are standardized by IPC.

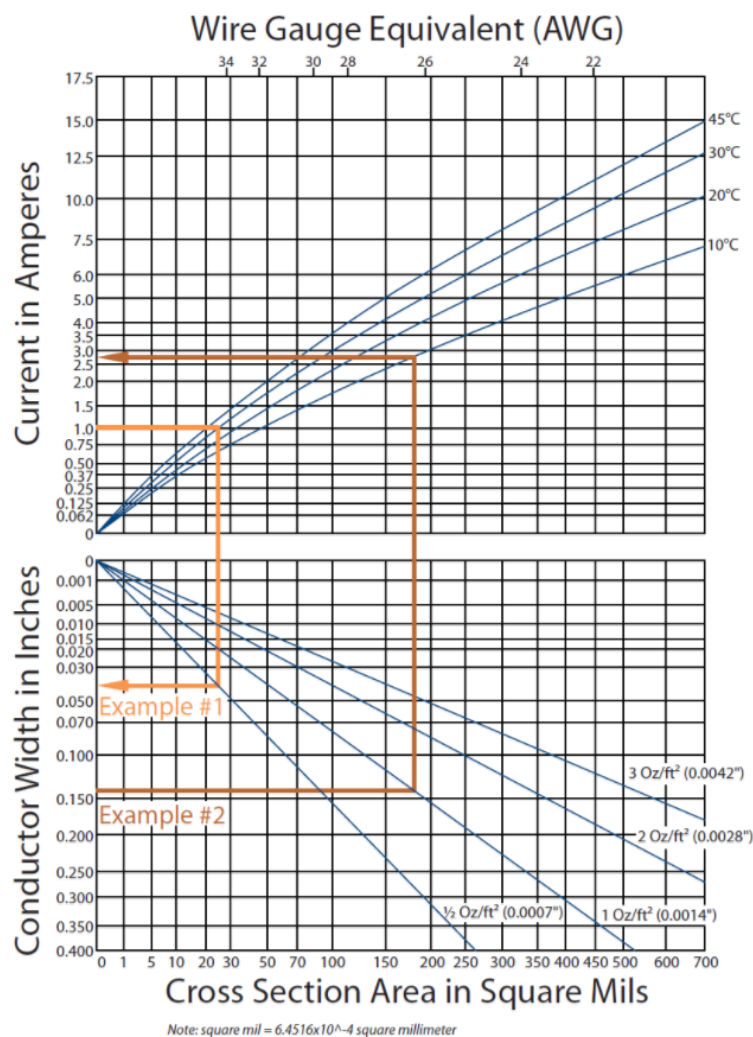


Figure 4.3. Relationship between cross section area and maximum current carrying capacity and temperature rise stated by IPC.

Figure 4.3 shows the calculation of thickness and width size of the copper trace with respect to temperature rise. If current in ampere is known in the system then, as the Example #1 shows, then the table tells the conductor width with respect to cross

section area. Also, the second example is done in the other way around. Thus, the trace size can be calculated by table and the temperature rise can be seen in the right side of the first graph. The maximum allowed temperature rise is defined by maximum sustained operating temperature of the PCB. On the other hand, making smaller PCB mostly depends on the size of chips, modules and connectors. Single side, double side or multilayer coppers are possible selections. However, it is sufficient to fabricate single side layer PCB in our study. There are different ways of masking copper plate.

In direct toner transfer method, the circuit should be printed out on a special paper for transferring toner on plate. While transferring toner on to copper plate, ironing or laminator may be used. However, if the temperature gets too high, toner gets liquid and traces will not appear. On the other hand, if the temperature is too low, toner will not stick on to copper plate. Since ironing sticks the paper on to plate, it is not easy to take the paper away. In photo-resistive method, the mask is printed out on a transparent paper and copper plate is coated with Pozitiv20 solution. The solution is sensitive to Ultra Violet (UV) light. Therefore, circuit design can be transferred onto the plate by masking it from UV light. Thus, UV light method has been chosen for the application.

4.2.1. UV Light Box

The box must emit UV light with 395 – 400nm wavelength to copper plate for masking application. UV Light Emitting Diode (LED) has been chosen for this box because it is cheap, powerful, efficient technology. Also, the other requirements for the application is suitable such as viewing angle, operating temperature, intensity etc. In the datasheet of chosen LED, it is stated that maximum current should be 30mA and forward voltage should be between 3.2 ~ 3.8V. Since 10cm * 22cm prototype PCB plate is going to be used for the project, the maximum number of LED should be placed considering power supply and circuitry for the LED driver. However, the adapter could supply 12V and maximum 2A current. As the LED forward voltage is around 3.2V, maximum three LEDs can be connected serially. Therefore, LEDs are connected by parallel with including 3 of them in the same line. This time the current

and size of the board creates the limitation. The parallel connection conducted by using this restriction. 36 parallel connection is available on the plate, so the total current on LEDs is calculated as 1.08A. The calculated voltage and ampere values can be supplied by the chosen adapter. While soldering the LEDs, $1\ \Omega$ and $\frac{1}{4}\ W$ resistors are added in each serial connection for equal current flow Figure 4.4.

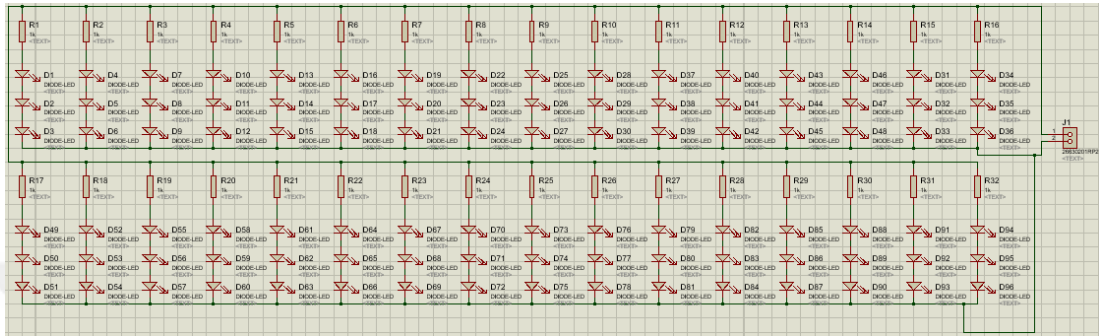


Figure 4.4. LED connection schematic.

Timing application is also important for exposing sufficient light to masked copper plate. Microcontroller, Liquid Crystal Display (LCD) and push-buttons should be added to circuit for adjusting exposure time. ATmega328p has been programmed for initialization of LCD, showing exposure time, push buttons and LED on-off switching. The Figure 4.6 shows the connection schematic of LCD and push buttons with microcontroller.

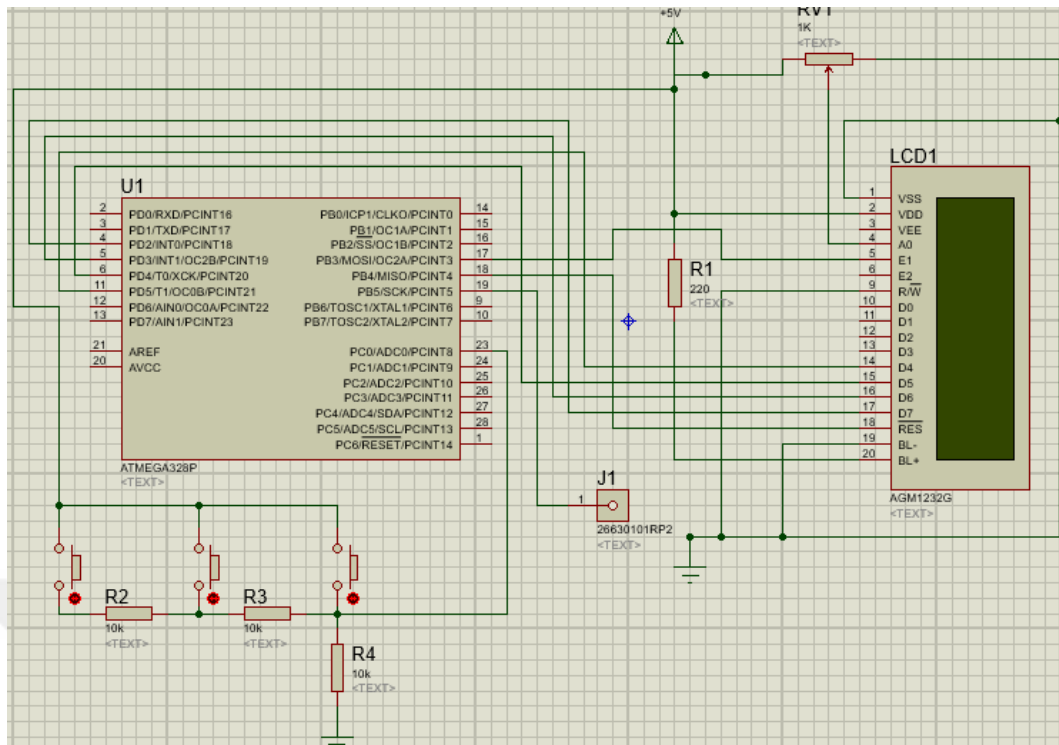


Figure 4.5. UV Box control unit design.

Each push button created by resistors outputs different analog values as seen in Figure 4.5. Therefore, each button can be assigned for different task which are incrementing/decrementing time and entering functions. Power, data lines, contrast adjusting, Read/Write, reset connections of LCD has been done. There needs to be circuit to supply the given stable current and time because microcontroller pin can only supply up to 40 mA. Since the led circuit needs 1.08 A current, the circuit is designed below (Figure 4.6).

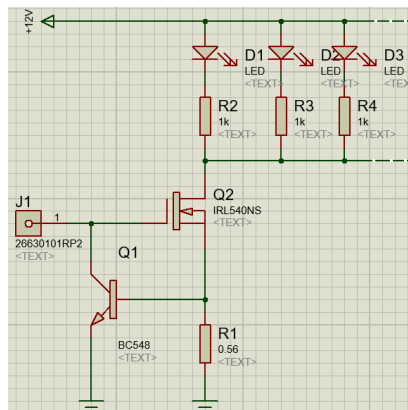


Figure 4.6. Designed LED driver circuit.

Logic level mosfet which is IRL540N has been chosen to control the current because the gate of the mosfet can be controlled via microcontroller. Thus, using microcontroller the user can select exposure time from LCD via buttons and can activate UV LEDs automatically. The activation stands for putting gate voltage of the mosfet high. The transfer characteristic of the mosfet (Figure 4.7) states that it is possible to open gate around 5V and draw current up to 60 A. On the other hand, the transistor BC548 controls the voltage on R₁ resistor, so the current is limited by chosen resistor value. The current value is going to be around 1.08 A and the voltage value of resistor is going to be around 0.58 ~ 0.70 V because of the base-emitter voltage of the transistor.

$$V = I \times R \tag{3.26}$$

Ohm's law shows that 0.6 Ω resistor is required for the circuit, but the calculated resistor type is not available on the market (Eq. 3.26). Therefore, the closest one which is 0.56 Ω has been chosen for the circuit. Changing resistor increases the current up to 1.16 A, so it is tolerable value on LEDs. Since LEDs are resistant up to 75 mA, the LEDs will continue to work. On the other hand, the power dissipation of the main resistor should be calculated before selecting power rating of it. Using power rule ($P = I \times V$), the power dissipation calculated as 0.75 W. Minimum 1 W rated 0.56 Ω resistor is the one that should be selected for the circuit.

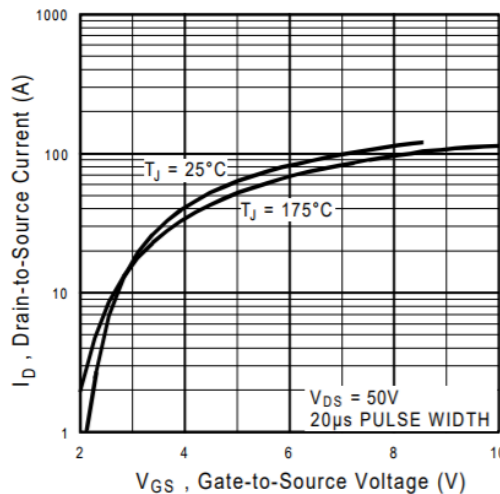


Figure 4.7. Typical transfer characteristics of IRL540N [24].

All the necessary materials have been supplied, gathered and put into box as seen in Figure 4.10(a). The drawings of anchor, tag and extension board for UWB module printed out with maximum resolution on to transparent paper. Copper plate must be clean before applying photosensitive lacquer. The solution should be sprayed on to board smoothly and plates should be allowed to dry about 24 hours in room temperature or 15 minutes in 75°C (Figure 4.8). Then, the drawing should be placed between the coated copper plate and high UV light (Figure 4.9). After exposure about 3 minutes of UV light, the plate is ready for etching process. The solution 7gr NaOH in 1L water should be developed and the plate should be put into it. The drawing should be seen on the copper plate after 3-4 minutes as seen in Figure 4.10(b). Lastly, etching should be completed with using FeCl₃. The remaining toner can be removed by acetone and the circuit is completed on the copper plate. Electrical connectivity should be tested before placing any component on the plate. The connectivity of traces can easily be checked by multimeter using short-circuit function. The developed PCBs can be seen in the Figure 4.11.

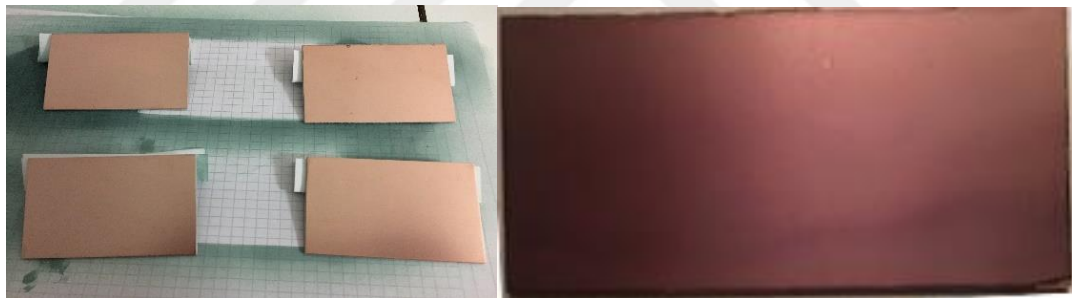


Figure 4.8. a) Clean copper plates b) Copper plate with dry photosensitive layer.

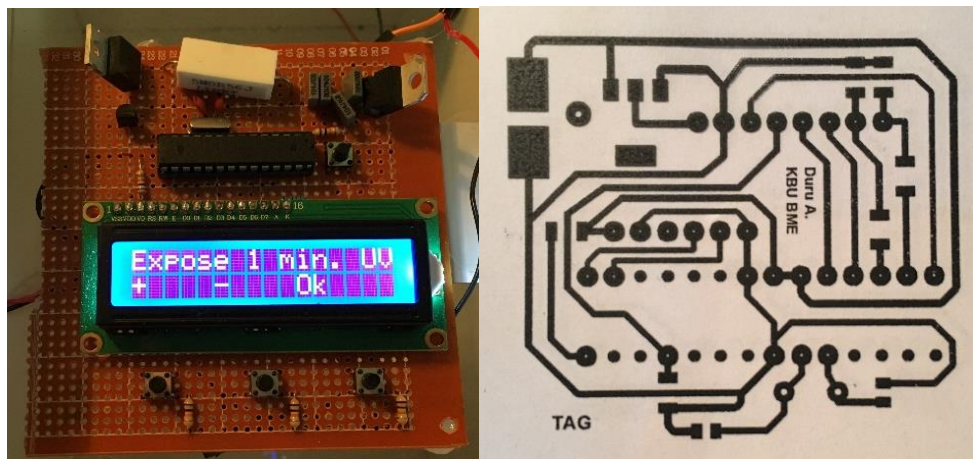


Figure 4.9. a) UV LED control unit b) Circuit drawing on transparent paper.

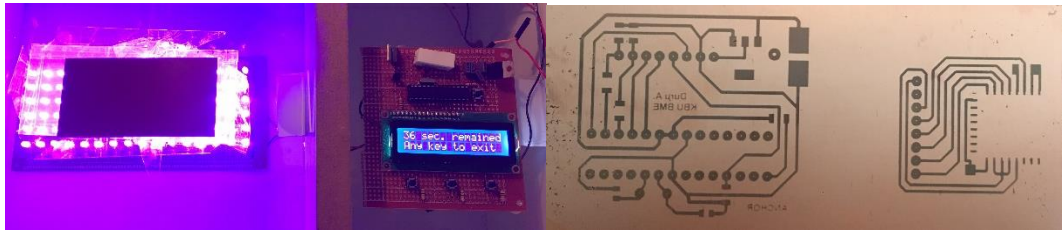


Figure 4.10. a) Circuit drawing exposure to the copper plate b) After NaOH application to the copper plate.

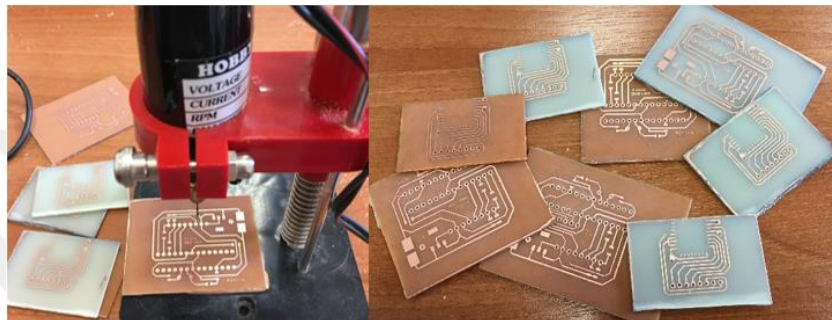


Figure 4.11. The PCBs after etching and drilling processes.

4.3. SOFTWARE DESIGN

Software must be designed considering requirements of the application. Anchors and tag were programmed with unique identifiers for the range measurements. Each MCU was equipped with necessary algorithms for configuration and communication between transceivers. Anchors, Tag and UV light box have been programmed by Arduino Integrated Development Environment (IDE). On the other hand, MATLAB [42] is used for getting data and solving algebraic problems and plotting required graphics.

4.3.1. Anchors and Tag

Reset Pin, IRQ Pin, SPI Select Pins are defined in the IDE. Device address, data transfer rate and power consumption mode is selected. Then, anchors will wait to get blink messages for measuring distance between devices. Tag is also programmed with similar definitions, but tag sends blink messages periodically and waits for

ranging initialization message. The anchors are reference points with respect to tag position.

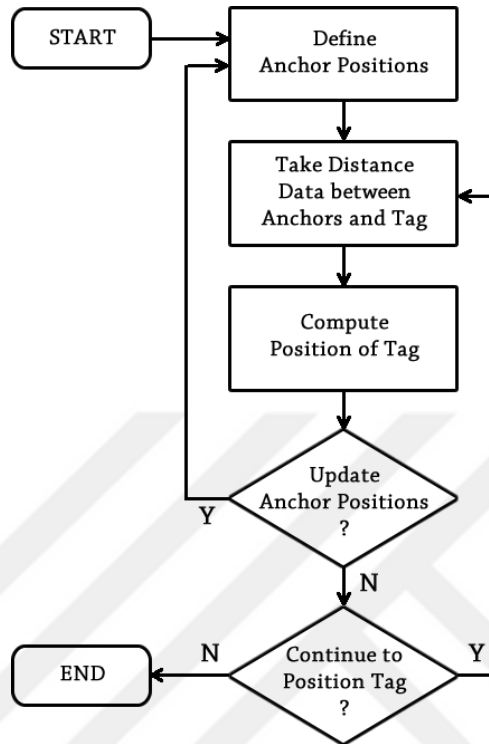


Figure 4.12. Flow chart of the algorithm.

At the beginning, anchors had to be placed in intended area and locations must be defined in the algorithm. After the initialization of MCUs, anchors will try to communicate with tag. When communication between transceivers starts, range estimation data will be available. These available measurements are going to be used to determine and draw the position of tag. If there is no anchor position update, then the system will continue to take measurements and estimate the position of tag. Figure 4.12 shows flow chart of the algorithm.

4.3.2. UV Light Box

LCD data pins and analog reading pin are defined. Then, number of columns and rows are defined to the microcontroller for printing message on the screen. “*Enter UV Exposure Time*” is written on LCD screen to get data input from user. When one of the three push buttons is pressed, three different analog values can be created. The

first button was programmed for increasing time, the second button was programmed for decreasing time and the third one was programmed for Enter button. Therefore, user can select the exposure time. In the program, the loop works with analog values by incrementing or decrementing an integer. When the enter button is pressed, the pin 13 will get in HIGH state and stay HIGH as long as the selected time has been counted by microcontroller. Making Pin 13 high will allow current to flow from the mosfet and it completes led driver circuit to work as long as the gate pin is HIGH.

4.3.3. Data Acquisition and Calculation

MATLAB is a numerical computing environment used for analyzing and designing systems. Distance data from microcontroller can be acquired with the program, so incoming distance measurements can be processed and plotted in real time. Reference points and incrementing operators are declared at the beginning of the program. The communication port and input buffer size has been chosen before the continuous distance measurement loop begins. The loop starts with opening the selected port and reading buffer data. The short addresses of anchors were programmed as static addresses. In this way, MATLAB can differentiate the address of incoming data to use in the algorithm. The range data is programmed and coming in the “f2r3.42” form. For instance, the start character which are “f2” defines the address of incoming data and “r3.42” defines range data which is 3.42m. Each iteration checks incoming character order in the loop and assigns distance value to related anchor. Since serial data is read one byte at a time, the incoming data should be converted to a string and range value must be converted to double for further calculations. Distance measurements are required to apply positioning algorithms. Trilateration, LSE, Centroid algorithms are implemented and measurements are taken in various positions. Moreover, algorithms for distance and position errors with respect to real position are developed. Thus, the system application of indoor positioning system is created.

CHAPTER 5

RESULTS AND DISCUSSION

This chapter provides information about performance of the designed system. The test results are presented for further discussion. Different positions are arranged and the data has been analyzed to test the accuracy of the system. Two UWB module has been used for distance tests because there should not be performance difference in each chip. If there is a big change between sensors then it can be concluded that there is a hardware problem. Basic offset calibration has been included in the algorithm. Position estimations with three different algorithms are presented. Error measurement results are given in the same graph to make comparison between them. Next, distance measurements and position estimation errors are discussed.

5.1. DISTANCE MEASUREMENT TESTS

Distance measurement tests use one tag and one anchor for data collection. First, distance measurements are held up to 5 m with 0.25 m steps. Then, 4, 6, 10, 15, 20-meter measurement tests have been conducted. The real distance was measured by laser meter having ± 2 mm accuracy. System accuracy has been tested and results show if there is drift occur over time. The Figure 5.1 shows the system setup for two-way ranging measurement.

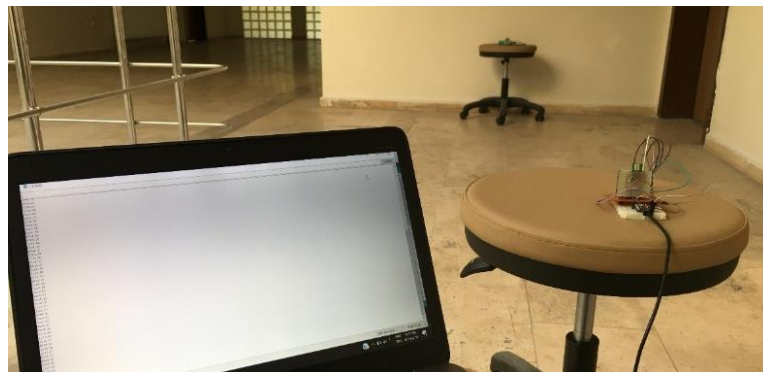


Figure 5.1. UWB based two-way communication system.

5.1.1. Measurements up to 5-meter

Distance measurements are held up to 5 m with 0.25 m steps for one anchor and one tag scenario. Real distance data are gathered by laser meter with $\pm 2\text{mm}$ precision. The system performance has been investigated in terms of standard deviation and the Mean Absolute Error (MAE). Standard deviation data indicates that how much data points differ from the mean value. Besides, the MAE measures the average magnitudes of the error. Position update rate for the test is 0.36 seconds per sample. 300 samples have been received for each step. Figure 5.2 shows standard deviation for each measurement and it has varied from 2.2 cm to 6.6 cm, with a mean value of 3.9 cm. Thus, it proves that the system gives useful and close estimations with respect to real distance. On the other hand, Figure 5.3 confirms that MAE is under 25 cm for a 50 cm or greater distance between transceivers. Average MAE has a value of 10 cm for the overall measurements.

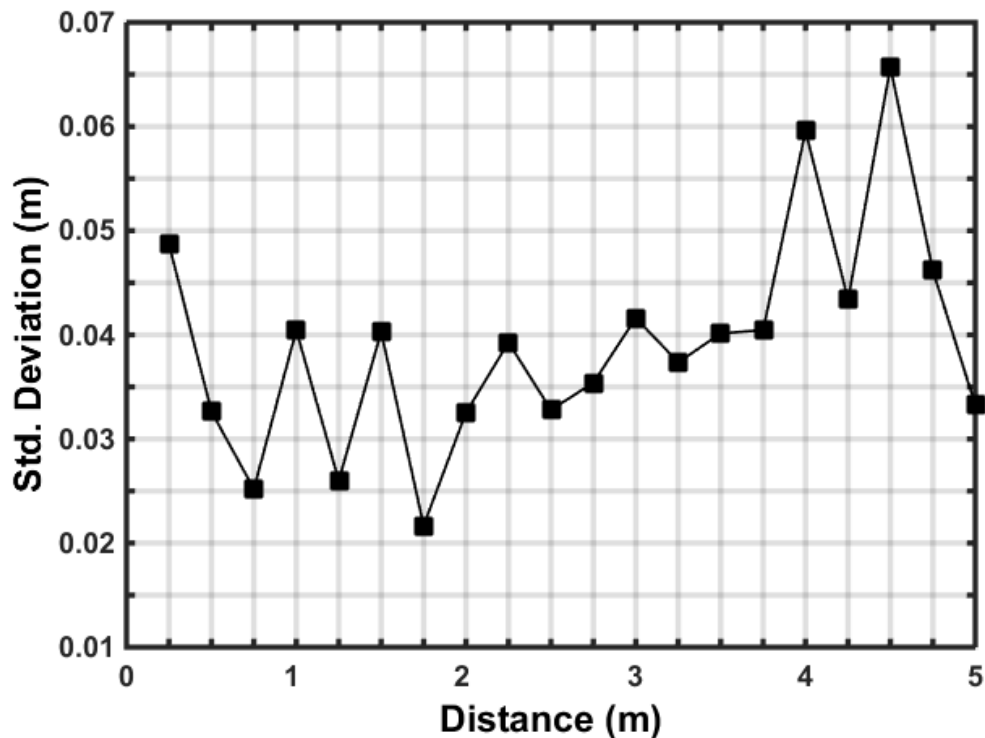


Figure 5.2. Standard deviation with respect to real distance.

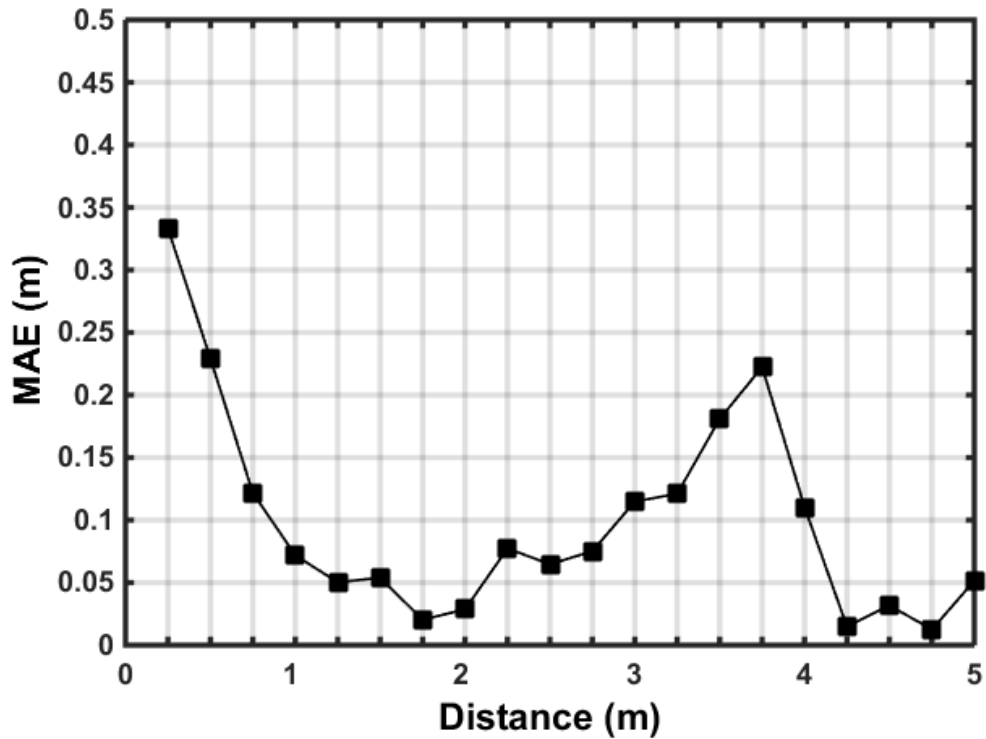


Figure 5.3. MAE with respect to real distance.

5.1.2. 4-meter measurement

Tag and anchor has been placed on top of stools. The distance between chips adjusted as 4 m with laser meter. Also, the distance between ground and chip measured to put sensors in same height. Although laser meter has ± 2 mm accuracy, the distance data has been taken three times to decrease user related error. Figure 5.4 shows the real distance between chips and the real distance between chip and ground.



Figure 5.4. Distance measurements between chips and ground with laser meter.

Figure 5.5 shows results of 4 m distance measurement test over 10 minutes. In addition, Figure 5.6 shows data sampling rate histogram with a mean of 0.3052

seconds per sample. Since mean of the samples is calculated as 4.696 m, -0.696 m offset calibration has been added to the provided data. Thus, minimum value has been found as 3.934 m and 4.094 m is acquired as maximum value with a standard deviation of 2.6 cm.

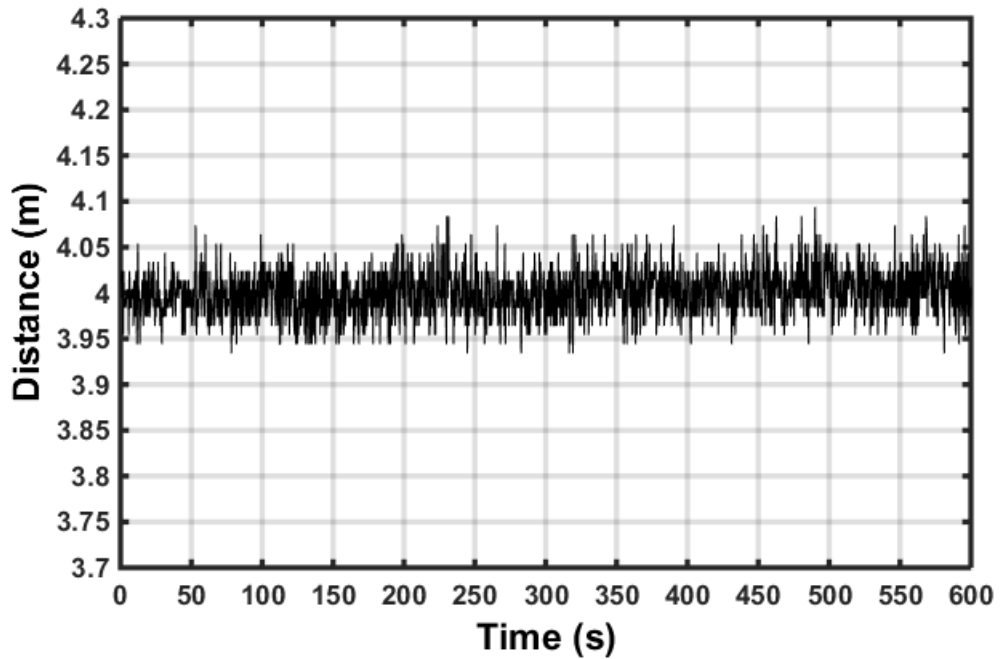


Figure 5.5. Results from 4-meter distance estimation test over time.

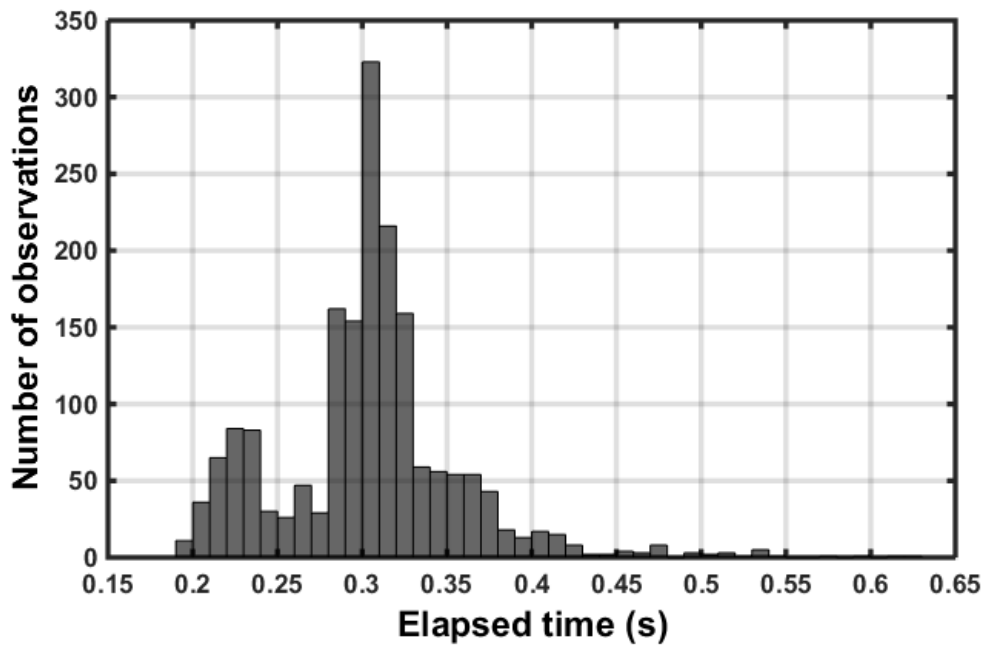


Figure 5.6. Elapsed time histogram for 4-meter distance estimation test.

5.1.3. 6-meter measurement

The distance between chips adjusted as 6m with laser meter. Although laser meter has ± 2 mm accuracy, the distance data has been taken three times to decrease user related error. Also, the distance between ground and chip measured to put sensors in same height. Figure 5.7 shows results of 6m distance measurement test over 10minutes. In addition, Figure 5.8 shows data sampling rate histogram with a mean of 0.2983 seconds per sample. Since mean of the samples is calculated as 6.611 m, - 0.611 m offset calibration has been added to the provided data. Thus, minimum value has been found as 5.919 m and 6.069 m is acquired as maximum value with a standard deviation of 2.3 cm.

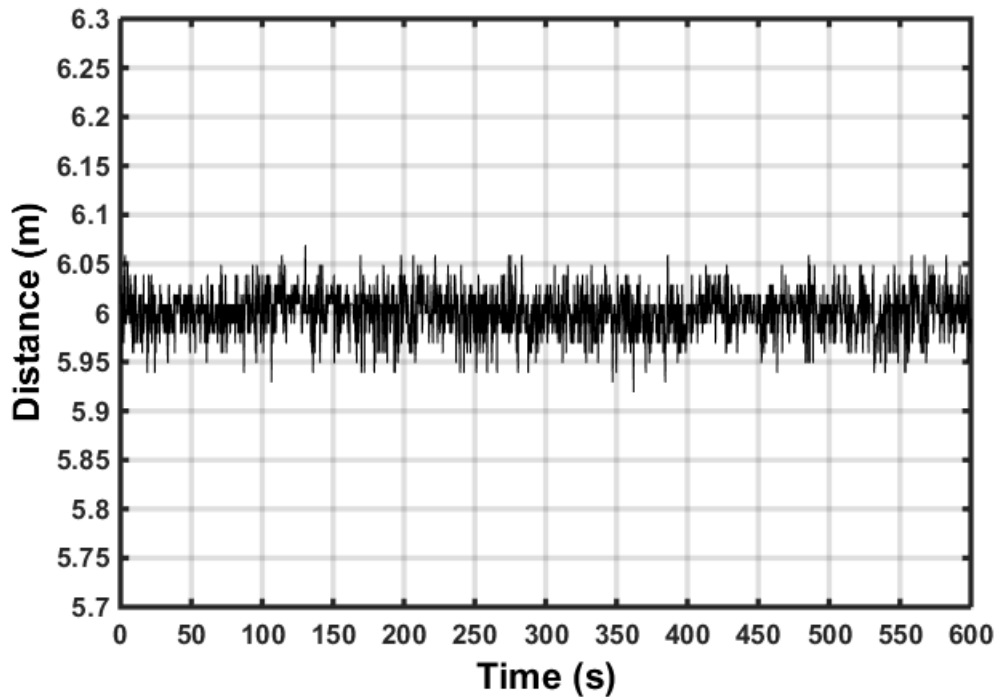


Figure 5.7. Results from 6-meter distance estimation test over time.

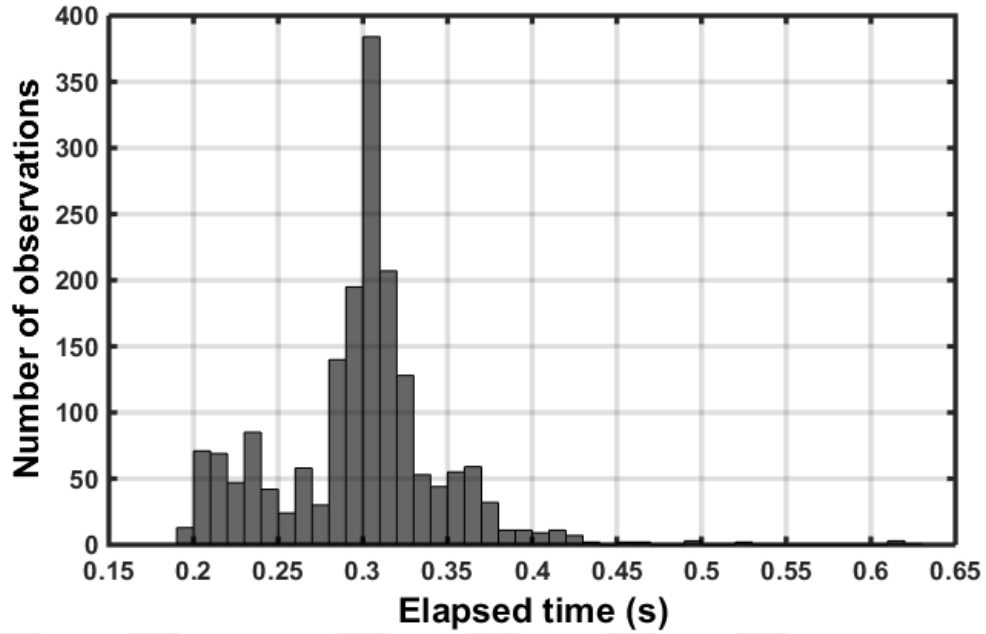


Figure 5.8 Elapsed time histogram for 6-meter distance estimation test.

5.1.4. 10-meter measurement

The distance between chips adjusted as 10m with laser meter. Although laser meter has ± 2 mm accuracy, the distance data has been taken three times to decrease user related error. Also, distance between ground and chip measured to put sensors in same height. Figure 5.9 shows results of 10 m distance measurement test over 10minutes. In addition, Figure 5.10 shows data sampling rate histogram with a mean of 0.3006 seconds per sample. Since mean of the samples is calculated as 10.81 m, -0.81 m offset calibration has been added to the provided data. Thus, minimum value has been found as 9.9 m and 10.08 m is acquired as maximum value with a standard deviation of 2.3 cm.

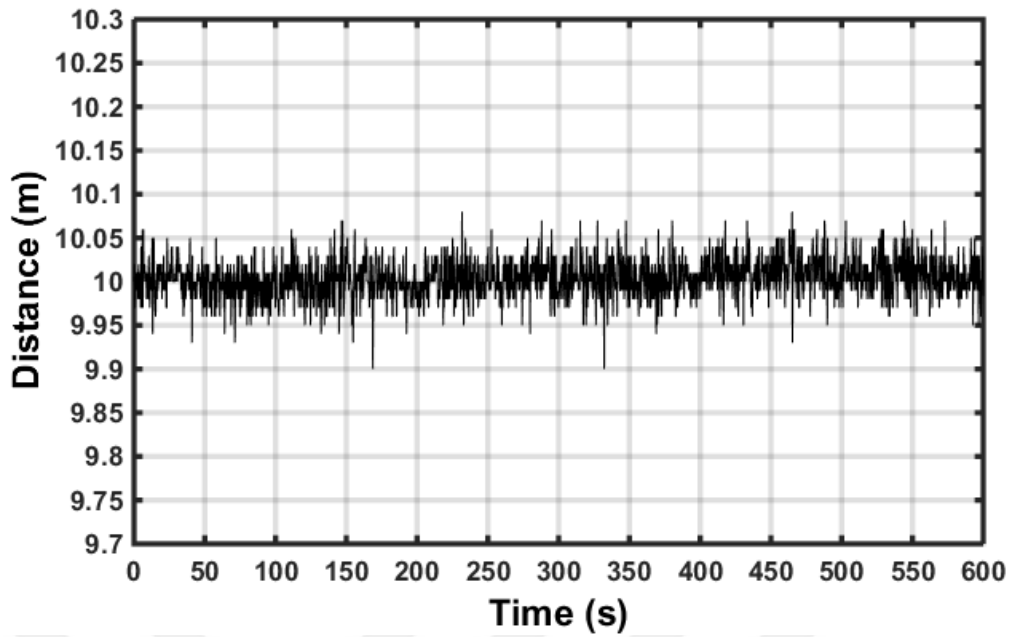


Figure 5.9. Results from 10-meter distance estimation test over time.

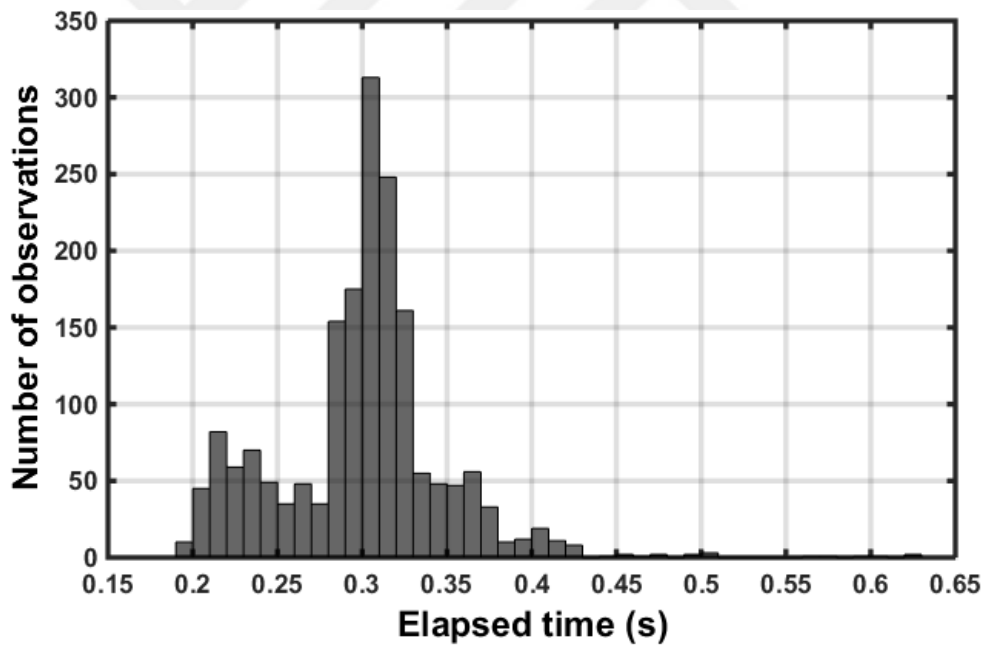


Figure 5.10. Elapsed time histogram for 10-meter distance estimation test.

5.1.5. 15-meter measurement

The distance between chips adjusted as 15 m with laser meter. Although laser meter has ± 2 mm accuracy, the distance data has been taken three times to decrease user related error. Also, the distance between ground and chip measured to put sensors in

same height. Figure 5.11 shows results of 15m distance measurement test over 10 minutes. In addition, Figure 5.12 shows data sampling rate histogram with a mean of 0.3014 seconds per sample. Since mean of the samples is calculated as 15.92 m, -0.92 m offset calibration has been added to the provided data. Thus, minimum value has been found as 14.91 m and 15.14 m is acquired as maximum value with a standard deviation of 3.4 cm.

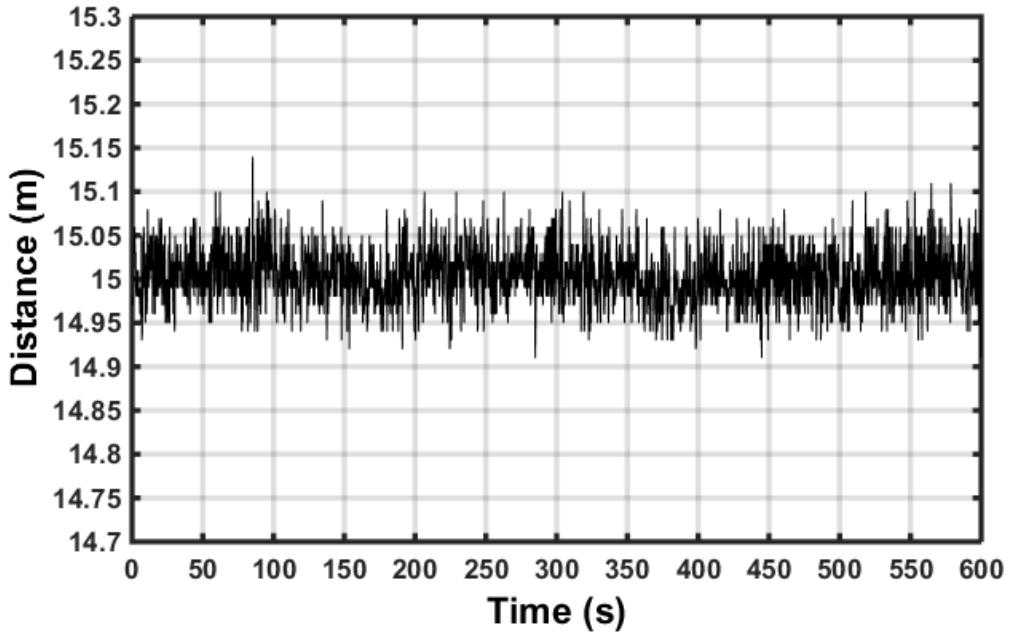


Figure 5.11. Results from 15-meter distance estimation test over time.

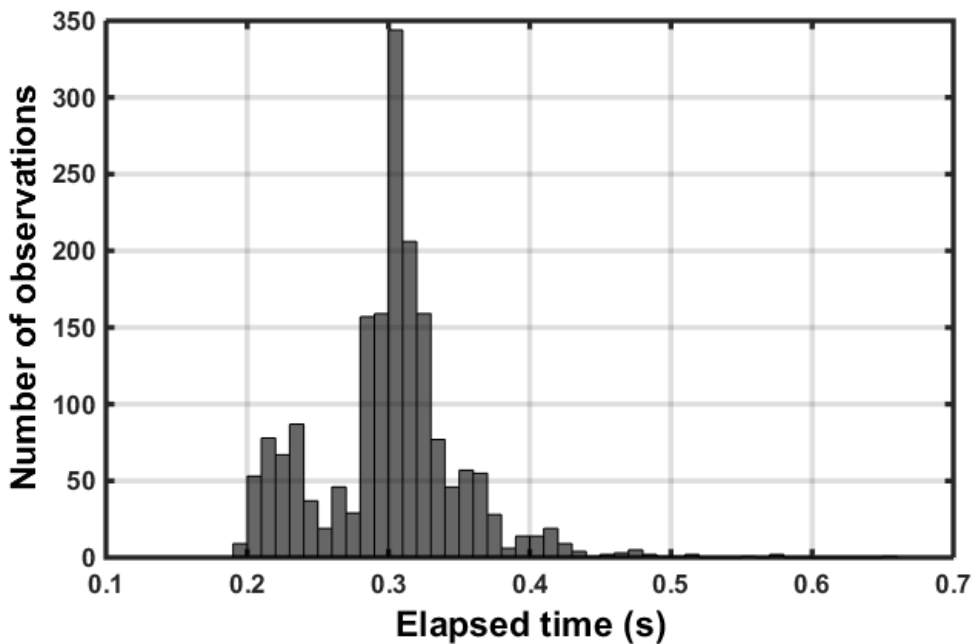


Figure 5.12. Elapsed time histogram for 15-meter distance estimation test.

5.1.6. 20-meter measurement

The distance between chips adjusted as 6 m with laser meter. Although laser meter has ± 2 mm accuracy, the distance data has been taken three times to decrease user related error. Also, the distance between ground and chip measured to put sensors in same height. Figure 5.13 shows results of 20 m distance measurement test over 10minutes. In addition, Figure 5.14 shows data sampling rate histogram with a mean of 0.3036 seconds per sample. Since mean of the samples is calculated as 20.79 m, - 0.79 m offset calibration has been added to the provided data. Thus, minimum value has been found as 19.87 m and 20.40 m is acquired as maximum value with a standard deviation of 5.7 cm.

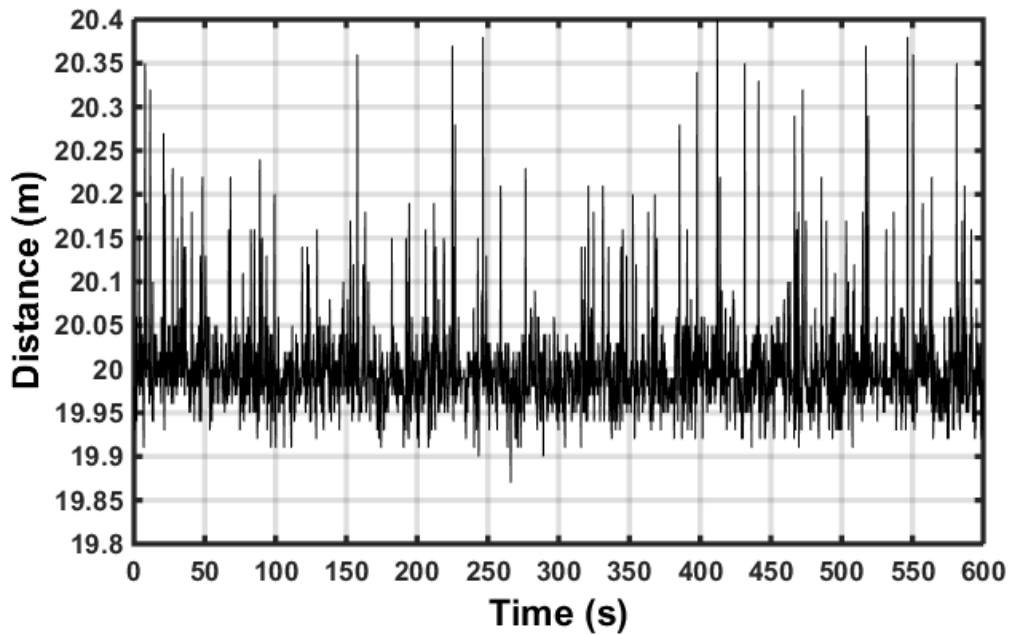


Figure 5.13. Results from 20-meter distance estimation test over time.

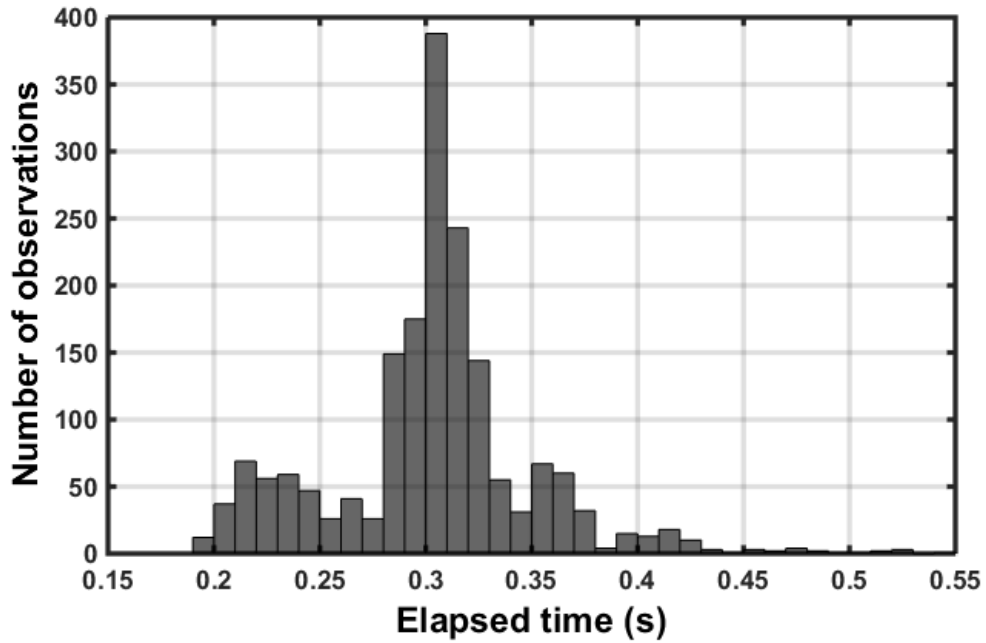


Figure 5.14. Elapsed time histogram for 20-meter distance estimation test.

Results are gathered to see the variation among values. Table 5.1 shows five different measurements with minimum, maximum, range, standard deviation properties. Minimum and maximum properties states peak data values in given test. Range is the difference between peak data measurements. Since mean data difference from real value has been calibrated, the offset value was stated. Standard deviation feature and MAE performance features are also added to the Table 5.1. Thus, results of measurement tests can be compared with given parameters.

Table 5.1. Distance measurement results.

	4-meters	6-meters	10-meters	15-meters	20-meters
<i>Min. (m)</i>	3.932 m	5.919 m	9.890 m	14.910 m	19.870 m
<i>Max. (m)</i>	4.092 m	6.069 m	10.080 m	15.140 m	20.400 m
<i>Range (m)</i>	0.160 m	0.150 m	0.190 m	0.230 m	0.530 m
<i>Offset (m)</i>	-0.698 m	-0.611 m	-0.810 m	-0.920 m	-0.790 m
<i>Standard dev. (cm)</i>	2.64 cm	2.28 cm	2.32 cm	3.37 cm	5.77 cm
<i>MAE (cm)</i>	2.14 cm	1.79 cm	1.83 cm	2.65 cm	3.67 cm

5.2. POSITION ESTIMATION

The simulation environment was chosen to apply three different positioning algorithms Trilateration, LSE and Centroid. The indoor area size was 4x11m and there were no obstacles to interfere signal transmission or LOS condition. The anchors were assumed to be randomly distributed at corners of the area. 3 anchors were placed for trilateration and centroid positioning algorithms. In LSE, 4 anchors were placed. Then, each positioning algorithm has been simulated to estimate position of tag with respect to real position. In each position, the algorithms were examined with 5 different random positions of tag. Results are given in Figure 5.15.

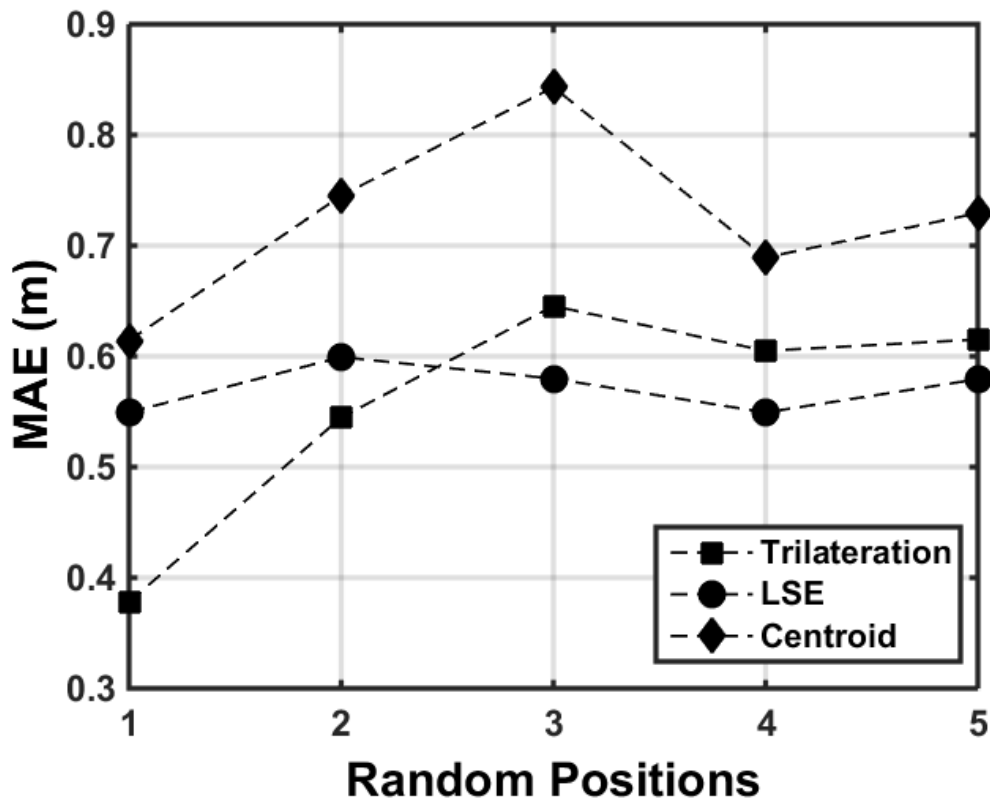


Figure 5.15. Positioning error with respect to random positions.

5.3. CONCLUSION

The measurements are carried out with different distances starting from 0.25 cm to 20 m. Results showed that range between minimum and maximum values stays less than 23 cm except for the 20 meters test. It can be concluded that transceivers can be

used up to 15 m to get good accuracy results. Also, offset value does not change much for all the measurements, but offset calibration must be done to converge correct distance. However, there are multiple error sources of measured data which can be explained. The primary source of error is antenna delay in hardware which cannot be controlled by user. The capacitance of the hardware may cause nanosecond level delays in transmission. The clock drift causes the distance measurement errors. Also, received signal level has effect on ranging accuracy. Increasing distance also returns worse results as in 20 meters test. Figure 5.13 shows larger peaks than the other tests which means there may communication problems in greater peaks. Thus, signal strength can be increased and better antenna must be used for larger positioning plans with minimum number of transceivers. Test results showed that UWB chips provide promising results, so the system can be applied for indoor positioning purposes. A system should be designed considering particular solutions for intended problem. By this way, performance trade-offs can be analyzed in better scope. Power efficiency, precision depends on focus of the project. If deployment price is not important than precision, then more complex hardware and software can be implemented for precise measurement. However, if desired system needs to be worn on body, then tag should be small, light-weight and consume low power. Although update rate affects the accuracy of the system, design should be small as much as possible and software must be implemented considering power consumption. All in all, intended use case of the system should be designed properly to get the best performance, so trade-offs must be kept in optimum level.

Cost of the created tags and anchors is relatively higher than other technologies because it is a new technology and there is very limited UWB chip manufacturers. Thus, large areas need more chips and it may not be a cost-effective solution. UWB technology can have variety of applications in biomedical area such as personnel tracking, medical equipment tracking. In this thesis, UWB technology for indoor positioning system has been implemented and 3 different lateration methods are applied. Implemented system can achieve positioning under 60 cm MAE with LSE. Applied positioning algorithms showed that LSE and trilateration algorithms have closer estimation rates than centroid method. The overall system accuracy gave very promising results for indoor positioning systems.

REFERENCES

1. Choliz, J., Hernandez-Solana, A., and Valdovinos, A., "Evaluation of algorithms for UWB indoor tracking", *Proceedings Of The 8th Workshop On Positioning Navigation And Communication 2011, WPNC 2011*, 143–148 (2011).
2. Dädeby, S., "A system for indoor positioning using ultra-wideband technology", M.S. Thesis, University of Gothenburg, Gothenburg, Sweden, (2017).
3. Dalveren, Y. and Kara, A., "Comparative Analysis of TDOA-based Localization Methods in the Presence of Sensor Position Errors TDOA-based Localization", 556–560 (2017).
4. Jiang, C. and Pan, J., "UWB based Positioning", M.S. Thesis, Lund University, Lund, Sweden, (2013).
5. Bouet, M. and Dos Santos, A. L., "RFID tags: Positioning principles and localization techniques", *2008 1st IFIP Wireless Days, WD 2008*, (2008).
6. He, S. and Chan, S. H. G., "Wi-Fi fingerprint-based indoor positioning: Recent advances and comparisons", *IEEE Communications Surveys And Tutorials*, 18 (1): 466–490 (2016).
7. Neburka, J., Tlamsa, Z., Benes, V., Polak, L., Kaller, O., Bolecek, L., Sebesta, J., and Kratochvil, T., "Study of the performance of RSSI based bluetooth smart indoor positioning", *2016 26th International Conference Radioelektronika, Radioelektronika 2016*, 121–125 (2016).
8. Larranaga, J., Muguiru, L., Lopez-Garde, J. M., and Vazquez, J. I., "An environment adaptive ZigBee-based indoor positioning algorithm", *2010 International Conference On Indoor Positioning And Indoor Navigation, IPIN 2010 - Conference Proceedings*, (September): 15–17 (2010).
9. Proskochylo, A., Vorobyov, A., Zriakhov, M., Kravchuk, A., Akulynichev, A., and Lukin, V., "Overview of wireless technologies for organizing sensor networks", *2015 2nd International Scientific-Practical Conference Problems Of Infocommunications Science And Technology, PIC S And T 2015 - Conference Proceedings*, 39–41 (2015).
10. Medina, C., Segura, J. C., and De la Torre, Á., "Ultrasound indoor positioning system based on a low-power wireless sensor network providing sub-centimeter accuracy", *Sensors (Switzerland)*, 13 (3): 3501–3526 (2013).

11. De Angelis, G., De Angelis, A., Moschitta, A., and Carbone, P., "Ultrasound based positioning using Time of Flight measurements and crosstalk mitigation", *Conference Record - IEEE Instrumentation And Measurement Technology Conference*, 2015–July1865–1870 (2015).
12. Quyum, A., "Guidelines for Indoor Positioning", M.S. Thesis, Lulea University of Technology, Lulea, Sweden, (2013).
13. Shchekotov, M., "Indoor localization methods based on Wi-Fi lateration and signal strength data collection", *Conference Of Open Innovation Association, FRUCT*, 2015–June (June): 186–191 (2015).
14. Norrdine, A., "An Algebraic Solution to the Multilateration Problem", *2012 Int. Conf. On Indoor Positioning And Indoor Navigation (IPIN)*, (April): 2012 (2012).
15. Zhang, J., Sahinoglu, Z., Kinney, P., "UWB Systems for Wireless Sensor Networks", *Proceedings of the IEEE*, 313-331 (2009).
16. Dhawale, M. M. R., Sarode, P. M. V and Nadiyana, P. H. B., "Communication and self location of Wireless Sensor Network or Nodes using Wireless System: A Survey", *Int. Journal of Application or Innovation in Engineering & Management*, 2 (4): 298–304 (2013).
17. Kuhn, M. J., Mahfouz, M. R., Turnmire, J., Wang, Y., and Fathy, A. E., "A multi-tag access scheme for indoor UWB localization systems used in medical environments", *2011 IEEE Topical Conference On Biomedical Wireless Technologies, Networks, And Sensing Systems*, 75–78 (2011).
18. "APPLICATION NOTE: APS013 APS013 APPLICATION NOTE The implementation of two-way ranging with the DW1000", 1–13 (2014).
19. Atmel, "ATmega48A/PA/88A/PA/168A/PA/328/P DataSheet", *AVR Microcontrollers*, 660 (2015).
20. "SPI Transfer Modes | USB-I2C/SPI/GPIO Interface Adapters", <http://dlnware.com/theory/SPI-Transfer-Modes> (2017).
21. "I2C Bus | USB-I2C/SPI/GPIO Interface Adapters", <http://dlnware.com/i2c> (2017).
22. Santoso, F. and Redmond, S. J., "Indoor location-aware medical systems for smart homecare and telehealth monitoring: state-of-the-art", *Physiological Measurement*, 36 (10): R53–R87 (2015).
23. decaWave, "ScenSor DWM1000 Module", DWM1000 IEEE 802.15.4 UWB Transceiver Module datasheet, (2015).
24. International Rectifier, "HEXFET Power MOSFETs", IRL540N datasheet, 51 (2017).

RESUME

Anday DURU was born in 1991 and he graduated elementary and high school education in Istanbul. Then, he started to study at Yeditepe University, Department of Biomedical Engineering in 2009. Then in 2014, he started assignment as a Research Assistant in Karabuk University – Biomedical Engineering Department. He is still pursuing his studies in wireless communication and positioning systems.

